Published online 13 June 2016

Nucleic Acids Research, 2016, Vol. 44, No. 17 ***8199–8215***
doi: 10.1093/nar/gkw535

The Shu complex promotes error-free tolerance of alkylation-induced base excision repair products

Stephen K. Godin[1], Zhuying Zhang[1,2], Benjamin W. Herken[1], James W. Westmoreland[3], Alison G. Lee[1], Michael J. Mihalevic[1], Zhongxun Yu[2,4], Robert W. Sobol[4,5], Michael A. Resnick[3] and Kara A. Bernstein[1,*]

[1]University of Pittsburgh School of Medicine, Department of Microbiology and Molecular Genetics, 5117 Centre Avenue, Pittsburgh, PA 15213, USA, [2]Tsinghua University School of Medicine, Tsinghua University, Haidian District, Beijing 100084, China, [3]Chromosome Stability Group, Laboratory of Molecular Genetics, National Institute of Environmental Health Sciences (NIEHS), National Institutes of Health, Research Triangle Park, NC 27709, USA, [4]Department of Pharmacology & Chemical Biology, Pittsburgh, PA 15217, USA and [5]University of South Alabama Mitchell Cancer Institute, 1660 Springhill Avenue, Mobile, AL 36604, USA

Received October 19, 2015; Revised May 31, 2016; Accepted June 02, 2016

ABSTRACT

Here, we investigate the role of the budding yeast Shu complex in promoting homologous recombination (HR) upon replication fork damage. We recently found that the Shu complex stimulates Rad51 filament formation during HR through its physical interactions with Rad55-Rad57. Unlike other HR factors, Shu complex mutants are primarily sensitive to replicative stress caused by MMS and not to more direct DNA breaks. Here, we uncover a novel role for the Shu complex in the repair of specific MMS-induced DNA lesions and elucidate the interplay between HR and translesion DNA synthesis. We find that the Shu complex promotes high-fidelity bypass of MMS-induced alkylation damage, such as N3-methyladenine, as well as bypassing the abasic sites generated after Mag1 removes N3-methyladenine lesions. Furthermore, we find that the Shu complex responds to ssDNA breaks generated in cells lacking the abasic site endonucleases. At each lesion, the Shu complex promotes Rad51-dependent HR as the primary repair/tolerance mechanism over error-prone translesion DNA polymerases. Together, our work demonstrates that the Shu complex's promotion of Rad51 pre-synaptic filaments is critical for high-fidelity bypass of multiple replication-blocking lesion.

INTRODUCTION

DNA double-strand breaks (DSBs) can arise from both endogenous sources such as cellular metabolites and DNA replication errors as well as from exogenous sources such as radiation and chemical exposure. Once a DSB occurs, the DNA ends can be processed for religation in a repair pathway called non-homologous end joining (NHEJ). Alternatively, the DSB ends are resected to create 3′ single-stranded DNA (ssDNA) overhangs that invade a homologous sequence as a repair template in a process called homologous recombination (HR). Use of the different DSB repair pathways depends on many different factors including the cell cycle stage (1), the DNA damage source and even the spatial relationship between the damaged DNA and its potential homologous donor (2,3). When DSBs are not accurately repaired then mutations, chromosomal rearrangements and even cell death can occur. Furthermore, mutations in genes important in DSB repair are associated with cancer predisposition and various syndromes including Bloom, Werner, Fanconi Anemia and Nijmegen breakage syndromes.

In budding yeast *Saccharomyces cerevisiae*, HR is the primary mechanism in the repair of DSBs and relies on Rad51 filament formation on the 3′ ssDNA ends (4). Not surprisingly, many proteins have evolved to regulate Rad51 filament formation and disassembly in order to temporally and spatially control HR (5–10). Rad51 filament formation depends upon the activities of Rad52 and its epistasis group of proteins, which include the Rad51 paralogues, Rad55–Rad57 (10–13). The precise mechanism of how Rad52 and Rad55–Rad57 enable Rad51 filaments to form is not completely understood. Recently it was uncovered that the Shu complex (also referred to as the PCSS complex) contains additional Rad51 paralogues (14–16) and is conserved in fission yeast and humans (17,18). The budding yeast Shu complex consists of four proteins, Shu1, Shu2, Psy3 and Csm2, where both Psy3 and Csm2 are structurally similar to each other as well as to Rad51 (14–17,19). We find that

*To whom correspondence should be addressed. Tel: +1 412 864 7742; Fax: +1 412 623 1010; Email: karab@pitt.edu

the Shu complex physically interacts with Rad51 through Rad55–Rad57, and acts to synergistically stimulate Rad51 filament formation when combined with the Rad51 regulators Rad52 and Rad55–Rad57 (10,20,21). In support of this model, in a direct repeat recombination assay, disruption of the Shu complex leads to a 50% reduction in spontaneous Rad51-mediated repair and a corresponding increase in Rad51-independent single-strand annealing (10,20). Other groups have found that Shu complex disruption leads to gross chromosomal rearrangements and to increased mutation frequency, which depends upon the translesion synthesis polymerases during post-replicative repair (19,21–23).

While disruption of many of the HR genes involved in Rad51 filament formation such as *RAD52* or *RAD55-RAD57* lead to sensitivity to a broad range of DNA damaging agents, Shu gene disrupted cells are primarily sensitive to DNA damage induced by methylmethane sulfonate (MMS). For example, whereas *rad52Δ* and *rad55Δ* cells are sensitive to ionizing radiation (IR), ultra-violet (UV) light and hydroxyurea (HU), Shu complex mutants are resistant to all these reagents (19,20,22,24). This observation has led us to propose that the Shu complex's role in HR may be restricted to the repair of specific types of DNA lesions, especially those that are created by MMS. However, what the nature of these MMS-induced lesions are and what the Shu complex role is in their repair remain unknown.

MMS is a DNA alkylating agent that methylates DNA, leading to adducts that slow replication forks, accumulation of ssDNA gaps behind the replication fork and potentially replication fork collapse (25). MMS specifically leads to N3-methyladenines (N3-MeA) and N7-methylguanines (N7-MeG) where N3-MeAs are thought to be directly toxic lesions that lead to altered replication fork dynamics (26,27). Other lesions can also occur upon MMS exposure including N3-methyl cytosines, which can be a source of hypermutability in ssDNA (28). DNA alkylation damage, such as that created by MMS exposure, is primarily repaired through the base excision repair (BER) pathway (Figure 1A; (29)). During BER in budding yeast, N3-MeA and N7-MeG DNA adducts are removed by the DNA *N*-glycosylase Mag1, which leaves an apyrimidinic/apurinic (AP) site in the DNA (30–33). Subsequently the Apn1 and Apn2 endonucleases nick the phosphodiester bond at the AP site resulting in a 5′ deoxyribose (5′-dRP) (Figure 1A, left side) (34–36). Then, DNA polymerase ϵ fills the gap and the flap endonuclease Rad27 removes the flap containing the 5′-dRP (37). Subsequently, the DNA backbone is sealed by DNA Ligase 1 (Lig1). In an alternative and less frequently used BER sub-pathway in budding yeast, the DNA glycosylase and AP lyase Ntg1 and its paralogue Ntg2 can nick the Mag1-generated AP site resulting in a 3′ deoxyribose (3′-dRP) (Figure 1A, right side)(34). This DNA intermediate can either be further processed by Apn1 and Apn2 or alternatively excised by the flap-endonuclease Rad1-Rad10. Subsequently, DNA polymerase ϵ fills the gap at the DNA damage site and then Lig1 completes repair. Although MMS-induced DNA damage is primarily repaired via BER, if the DNA damage occurs during replication then partial processing of the damage can lead to replication fork stalling, the accumulation of ssDNA gaps and fork collapse (38). It is these types of lesions that are then targeted for repair/bypass by HR. How HR responds to BER intermediates encountered by a replication fork during DNA replication is not well understood but is thought to depend upon the DNA repair proteins Mre11-Rad50-Xrs2 as well as Rad51 and Rad52 (38).

Here, we show that the Shu complex mutant cells are additionally sensitive to high doses of camptothecin (CPT), which is a Top1 inhibitor that results in ssDNA breaks that lead to replication fork collapse and one-ended DSBs. Since BER of MMS-induced DNA lesions can also produce ssDNA breaks, this finding raised the question as to what specific DNA lesion(s) produced by MMS are acted upon by the Shu complex. To pinpoint which DNA intermediates produced during BER are acted on by the Shu complex, we generated different BER mutants that block repair of alkylated DNA at specific intermediates, such as abasic sites or 3′-dRPs, and screened for synthetic sensitivity with disruption of the Shu complex gene *CSM2*. Using this genetic approach, we find that upon exposure to MMS, *csm2Δ* cells are synthetically sick when combined with *mag1Δ* or *apn1Δ apn2Δ* disruptions at low doses of MMS, and that these cells exhibit elevated mutagenesis, altered recombination, impaired progression through S phase, and a heightened reliance upon translesion synthesis DNA polymerases. In addition, we observe a synthetic interaction in *csm2Δ rad27Δ* cells, and find that this synthetic growth defect is suppressed by over-expression of human DNA polymerase β (Polβ). Together, our work expands upon the types of lesions the Shu complex is known to act on in the context of both endogenous and MMS-induced replicative stress and provides evidence that the lethality caused by MMS is due to a spectrum of lesions that exist concurrently in a replicating cell.

MATERIALS AND METHODS

Strains, plasmids and media

The strains and plasmids utilized here are listed in Supplementary Table S1. All the yeast strains are RAD5+ and isogenic to W303 W9100-2D. Yeast crosses, transformations and tetrad dissections were conducted as described (39). Similarly, the media preparation was done as described except with twice the amount of leucine added (39). MMS (0.002%, 0.006%, 0.012%, 0.02%, Sigma 129925), hydroxyurea (100 mM HU; Sigma H8627), hydrogen peroxide (3 mM H_2O_2; Fisher H323-500), camptothecin (50 μg/ml CPT; Sigma C9911) and etoposide (2 mM; Sigma E1383) were added to YPD medium at the indicated final concentrations. Cisplatin (40 μg/ml; Sigma ALX-400-040-M250) was made in SC medium. CPT (10 mg/ml), cisplatin (100 mg/ml) and etoposide (50 mM/ml) stock solutions were re-suspended in di-methyl sulfoxide (DMSO). The primers used to make the specific gene knockouts are listed in Supplementary Table S2. *APN1* and *APN2* genes were disrupted with a hygromycin cassette (pFA6a-hphNT1) using the indicated S1 and S2 primers as described (40). *NTG1* and *NTG2* genes were disrupted with a clonat cassette (pFA6a-natNT2) using the indicated S1 and S2 primers as described (40). *MAG1* were disrupted with histidine using the pFA6a-His3MX6 cassette and the indicated S1

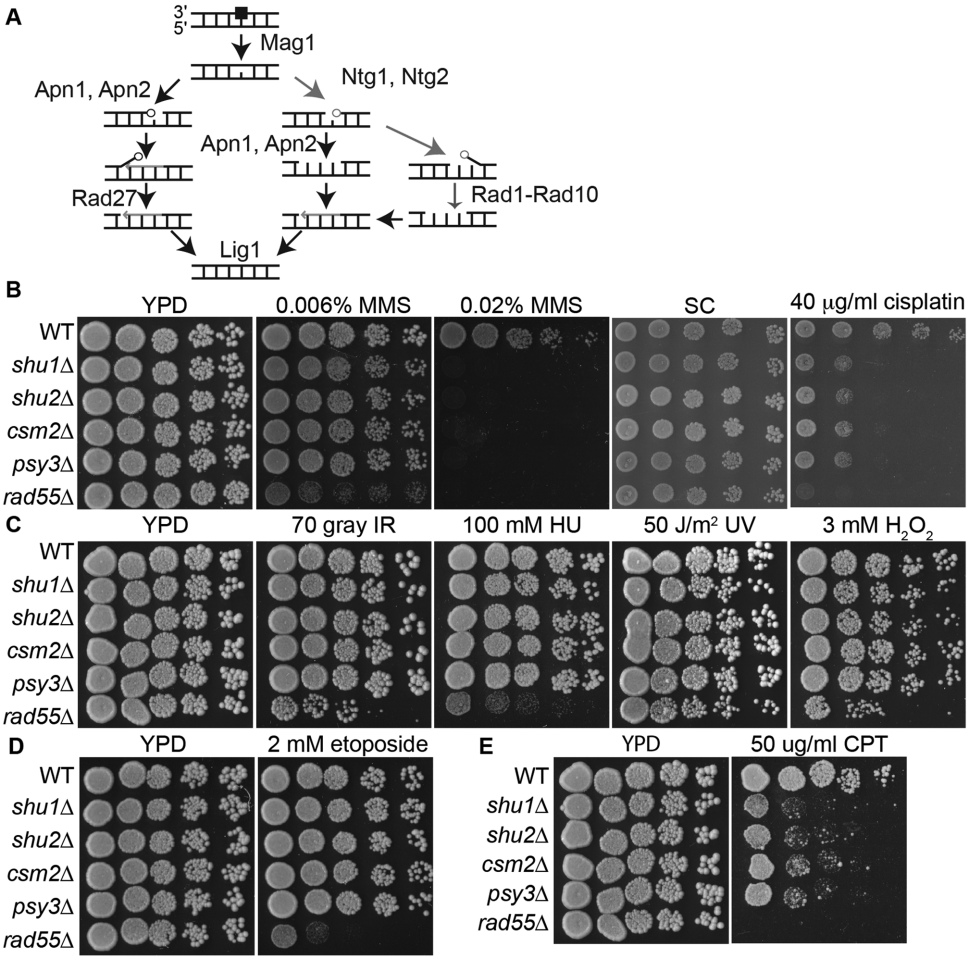

Figure 1. Schematic of base excision repair (BER) and the Shu complex primary sensitivity to methylmethane sulfonate (MMS) induced DNA damage. (**A**) Cartoon of BER pathway adapted from (51). The black arrows indicate the major pathway. (**B**) The indicated strains were 5-fold serially diluted onto YPD medium, YPD medium containing 0.006% or 0.02% MMS, SC medium or SC medium containing 40 μg/ml cisplatin. The plates were incubated for two days at 30°C and photographed. (**C**) Same as (B) except that the YPD plate was exposed to 70 Gray ionizing radiation (IR) or 50 J/m^2 ultra-violet (UV), or contained 100 mM hydroxyurea (HU) or 3 mM H_2O_2. (**D**) Same as (B) except that 2 mM etoposide was added to the YPD medium. (**E**) Same as (B) except that 50 μg/ml CPT was added to the YPD medium.

and S2 primers as described (41). Polymerase chain reaction (PCR) colony amplification and genotyping of *APN1, APN2, NTG1, NTG2, MAG1* was done using the indicated primers in Supplementary Table S2. The Polβ expression vector was made using the gateway cloning system and sub-cloned into the constitutive pAG414-GPD or galactose inducible pAG414-GAL-ccdB plasmid (Addgene plasmids #14144 and #14143 from Susan Lindquist), which contains *TRP1* and Ampicillin selectable markers for yeast and bacteria, respectively.

Growth assays

Yeast strains were incubated in 5 ml YPD medium overnight at 30°C and then diluted to 5 ml OD_{600} 0.2. The cultures were incubated for another 3 h at 30°C and equal cell numbers (5 μl of culture at OD_{600} 0.5) were 5-fold serially diluted onto YPD medium or YPD medium containing 0.002%, 0.006%, 0.012% or 0.02% MMS as indicated. The plates were incubated at 30°C for 2 days and photographed. To examine yeast with Polβ over-expression, the indicated yeast strains were transformed with pAG414-GPD or pAG414-GAL empty or Polβ expressing plasmids. The yeast were grown on minimal SC medium lacking tryptophan overnight at 30°C and then 5-fold serially diluted on YPR + GAL (containing 2% raffinose and galactose) with or without 0.02% MMS or to YPD medium with 0.002% or 0.006% MMS.

Canavanine mutagenesis assay

Three to seven individual *CAN1* colonies of wild-type (WT), *csm2Δ*, *apn1Δ apn2Δ*, *csm2Δapn1Δ apn2Δ*, *csm2Δntg1Δ ntg2Δ*, *ntg1Δ ntg2Δ*, *mag1Δ*, *csm2Δ mag1Δ*, *rad5Δ*, *csm2Δ rad5Δ*, *ubc13Δ*, and *csm2Δ ubc13Δ* were grown in 5 ml of YPD medium or YPD medium containing 0.002% MMS (18 h) overnight at 30°C to saturation. The cultures were diluted 100 000-fold and 120 μl was plated onto SC medium or diluted 10-fold and 250 μl was plated onto SC-ARG+CAN medium. The plates were incubated for 2 days at 30°C. Colonies were then counted to measure forward mutation frequency (SC-ARG+CAN) or total

cell number (SC). For each trial, a median frequency was obtained and an average of each trial median was reported. The experiment was repeated three to four times with standard deviations plotted on the graph and significance determined by Student's *t*-test.

Recombination assay

Mitotic recombination assays were performed as described (20). Briefly, nine independent colonies for each strain were grown up overnight at 30°C in 2 ml of SC with or without MMS before being diluted to OD_{600} 0.1. A total of 250 μl of this OD_{600} 0.1 culture was plated onto SC-LEU plates to capture recombination events. The OD_{600} 0.1 culture was further diluted 1:1000 before 250 μl were plated onto SC plates to calculate viable cells. After two days of growth, colonies were counted and the SC-LEU plates were replica plated onto SC-URA and 5′-FOA to observe Rad51-dependent and independent recombination events, respectively. Recombination rates and standard deviations were calculated as described (42) using the online FALCOR analysis tool (43).

Microscopic analysis

Cells were inoculated into 5 ml SC+ADE as described (20) and grown up overnight at room temperature. Cells were diluted 1:10 and allowed to grow for 3 h prior to imaging. Cells were imaged as an 11-step Z-stack with 0.3 μM per step. RAD52-YFP was visualized at 600 ms per image and RFA1-CFP was visualized at 500 ms. The results shown are the average of three individual experiments where at least 100 cells were imaged per strain per trial.

Protein level analysis

Logarithmically growing cells were arrested with 10 μmol alpha factor for 3 h, then released into room temperature YPD. At the indicated time points, equal cell numbers (1 OD_{600}) was removed and TCA prepped and run on a 10% SDS-page gel as previously described (44) where the Kar2 (Santa Cruz sc-33630) and HA antibodies (Roche 12CA5) were used at 1:1000 dilution.

Pulse-field gel electrophoresis analysis

The 50 ml cultures of each indicated strain at OD_{600} 1 were G2-arrested for 3 h with 1.5 μg/ml nocodazole. After 3 h, the cells were pelleted and resuspended in 40 ml of phosphate buffered saline (PBS) with 0.1% MMS at 30°C with shaking for 15 min. At 15 min, 40 ml of 10% sodium thiosulfate was added to each culture to inactivate the MMS, and then the cells were pelleted, washed once in YPD medium, and then resuspended in 25 ml YPD containing 1.5 μg/ml nocodazole. A total of 125 μl of 1.5 mg/ml nocodazole was added at 2.5 and 5 h to maintain G2 arrest. Equal cell numbers (3 OD_{600}) were harvested just prior to MMS treatment for the control sample, and at T = 0, 1, 2, 4, 6 and 8 h following MMS exposure. After harvesting, the cells were washed once in ice cold buffer V (100 mM EDTA, 50 mM Tris pH 7.4) and kept on ice until being made into plugs for PFGE analysis. To make plugs, the cells were briefly warmed at 42°C, resuspended in 100 μl of 0.5% agarose with zymolyase and cast using a biorad plug mold. Plugs were incubated in buffer V for 30 min at 37°C to allow cell wall digestion and then incubated overnight in 1% Tween with 1 mg/ml Proteinase K to lyse cells. Alternatively, for the S-phase progression experiments, logarithmically growing cells were arrested by alpha factor addition for 3 h, released into fresh YPD for 10 min and then treated with 0.033% MMS for 1 h before being washed and resuspended in YPD to start the time course experiment as previously described (45). PFGE was carried out with a CHEF Mapper (BioRad) using the following conditions: 10–90 s pulses ramped linearly for 24 h at 6 V/cm using 120° pulse angle at 14°C.

RESULTS

Disruption of the Shu complex genes lead to sensitivity to MMS, CPT and cisplatin but not to DNA damaging agents such as IR, HU, UV, H_2O_2 or etoposide

To determine the types of DNA lesions that the Shu complex responds to we sought to directly compare the sensitivity of Shu complex mutants (*shu1Δ, shu2Δ, csm2Δ* and *psy3Δ*) and the Rad51 paralogue *rad55Δ,* to a broad range of DNA damaging agents (Figure 1B–E). Using this approach, DSBs are predicted to form after exposure to IR, MMS (leading to replication fork slowing and collapse or DSBs derived from processing closely opposed lesions), HU (which limits dNTP pools leading to replication fork stalling and collapse), CPT and etoposide (which is a Top2 inhibitor that leads to single- and double-strand breaks). In addition, we analyzed cells for sensitivity to acute UV exposure (primarily thymine dimers), cisplatin (principally intra-strand crosslinks) and hydrogen peroxide (oxidative damage). By serial dilution, as a positive control we confirmed that Shu complex mutants are primarily sensitive to MMS (19,20,22,24), which can cause DSBs and replicative collapse, and not to direct DSB-inducing agents such as IR or etoposide, or replicative stalling agents such as HU (Figure 1B–D) (19,22,24). Interestingly, Psy3 (Platinum Sensitivity 3) was originally identified and named in a genome-wide screen for its sensitivity to oxaliplatin and cisplatin, both drugs that create inter- and intra-strand DNA crosslinks (46). Here, we demonstrate that the rest of the Shu complex mutants, *shu1Δ*, *shu2Δ* and *csm2Δ* are also identically sensitive to cisplatin (Figure 1B).

We do not observe sensitivity of Shu complex mutants to UV or H_20_2 (Figure 1C), although we can not rule out that chronic exposure to UV, which increases reliance upon bypass mechanisms, would cause sensitivity in a Shu complex mutant cell. Finally, we find that *rad55Δ* cells display increased sensitivity to MMS as well as to a broader range of DNA damaging agents (i.e. cisplatin, IR, HU, etoposide, CPT) than the Shu complex mutants (Figure 1B–E). Interestingly, we also find that the Shu complex mutants exhibit a mild sensitivity to high doses of CPT, a Topoisomerase I inhibitor that leads to the formation of excess ssDNA breaks that are channeled into DSBs at a replication fork (Figure 1E). This finding suggests that the Shu complex may contribute to the repair of one-ended DSBs formed by high

doses of CPT at a replication fork. Previous work has suggested that the Shu complex responds to the direct replicative blocks produced by MMS, such as N3-MeAs, but the finding that Shu complex mutants are sensitive to the ssDNA breaks produced by CPT suggest that the Shu complex could be capable of promoting repair of ssDNA breaks produced as intermediates during BER (47).

Upon MMS exposure, the Shu complex mutants exhibit synthetic sensitivity when combined with *mag1Δ*

To understand the role of the Shu complex in the tolerance of MMS-induced DNA lesions, we combined Shu complex mutants with disruption of BER genes and tested these mutants for synthetic sensitivity upon MMS exposure. Since Mag1 is necessary for processing DNA damage into AP sites and its disruption would block downstream processing of the MMS-induced DNA damage, we began our analysis with *mag1Δ* cells, which accumulate methylated DNA adducts such as N3-MeAs upon MMS treatment (Figure 2A). When compared to WT, *mag1Δ* cells are sensitive to 0.012% MMS whereas *csm2Δ, shu1Δ, shu2Δ* and *psy3Δ* cells are sensitive to 0.02% MMS (Figure 2B, Supplementary Figure S1). Consistent with a previous study (47), we observe a synthetic sensitivity when *mag1Δ* is combined with disruption of any of the Shu complex genes (*csm2Δ, shu1Δ, shu2Δ, psy3Δ*)(0.006% MMS, Figure 2B, Supplementary Figure S1). Furthermore, the synthetic sensitivity on low dose MMS of the double *mag1Δ shuΔ* mutants is equivalent regardless of which Shu complex component is disrupted (Figure 2B, Supplementary Figure S1). The Shu complex functions as an obligate heterotetramer where Csm2 confers DNA binding activity and most of the physical interactions between the Shu complex and other HR proteins occur through this subunit (15,16,20,21). Therefore, we focused on *csm2Δ* cells for the rest of our analysis.

csm2Δ mag1Δ cells exhibit elevated mutation frequencies and recombination rates upon MMS exposure

Disruption of the Shu complex mutants results in increased mutation frequencies that are measured by analyzing cells for mutations in the arginine permease gene (*CAN1*)(19,22). WT *CAN1* cells die when grown in the presence of canavanine; however, mutations in *CAN1* prevent this lethality and can readily be scored by plating on medium containing canavanine. To determine how the un-excised MMS damage contributes to the increased mutations observed in *csm2Δ* cells, we analyzed the *csm2Δ mag1Δ* cells for spontaneous and MMS-induced mutations in the *CAN1* gene (Figure 2C). *csm2Δ* cells, like other HR mutants, have an elevated basal mutation frequency compared to WT cells (Figure 2C) that is exacerbated by growth in low dose MMS (Figure 2C) (19,22). Interestingly, we do not observe an increase in the mutation frequency of *mag1Δ* cells compared to WT in the absence of MMS, although a modest increase is evident in MMS-treated *mag1Δ* cells (Figure 2C, $P < 0.05$). Although spontaneous mutation frequencies in untreated *csm2Δ mag1Δ* are similar to the *csm2Δ* single mutant (Figure 2C; $P > 0.5$), upon MMS exposure we observe a synergistic increase in mutation frequency comparing the *csm2Δ* and *csm2Δ mag1Δ* mutants (Figure 2C, $P < 0.05$ comparing *csm2Δ* and *csm2Δ mag1Δ* after MMS treatment). Due to the high sensitivity of *csm2Δ mag1Δ* cells, chronic low-dose MMS exposure was used in liquid culture experiments to maintain viability of the double mutants. These results suggest that in the absence of *MAG1*, the Shu complex contributes to high-fidelity bypass of alkylated DNA.

To test the hypothesis that MMS lesions are bypassed using high-fidelity mechanisms such as HR, rather than error-prone TLS, we examined MMS-treated *mag1Δ* cells for increased recombination rates (48,49). To do this, we utilized a direct repeat recombination assay that enabled us to measure total recombination rates as well as the type of recombination events that occurred. As pictured (Figure 2D), recombination events that produce a *LEU2* allele can occur via Rad51-dependent gene conversion (GC), which retains the *URA3* allele, or by Rad51-independent single-strand annealing (SSA) where the intervening *URA3* allele is deleted. SSA is usually considered to require a break, as the DNA needs to be resected back to reveal homology between the two *LEU2* alleles. Alternatively, it has been shown using a similar assay that SSA-like colonies can be generated by a Rad51-independent, inter-sister recombination event (50). Consistent with our hypothesis that HR bypasses the majority of the MMS-induced lesions, we find that MMS treated WT and *mag1Δ* cells exhibit a 3- to 4-fold induction in recombination rates (Figure 2D, P value < 0.05). Interestingly, the MMS treated WT and *mag1Δ* cells have a significant bias toward Rad51-mediated GC that is dependent upon *CSM2* (Figure 2E, compare WT to *csm2Δ*, $P < 0.005$ and *mag1Δ* to *csm2Δ mag1Δ* $P < 0.001$). This unexpected finding indicates that MMS-induced lesions are preferentially channeled into Rad51-dependent GC, whereas spontaneous lesions do not show any bias in the HR pathway (Figure 2E, compare untreated and treated WT). Surprisingly, we also find that the accumulation of lesions in MMS-treated *mag1Δ* cells also leads to a significant increase in SSA relative to treated WT cells (Figure 2E, P value < 0.05). Together, these data suggest that the majority of MMS lesions encountered by a replication fork are channeled into high-fidelity mechanisms of damage tolerance and bypass.

CSM2 disrupted cells exhibit a synthetic sensitivity with *apn1Δ apn2Δ* upon MMS exposure

Since we observe a synthetic MMS sensitivity between the Shu complex mutant *csm2Δ* and *mag1Δ*, we asked whether this phenotype is due to a general defect in BER, an accumulation of methylated DNA, or to the accumulation of specific BER intermediates. To address this question, we first determined if disruption of the down-stream AP site processing factors, *APN1* or *APN2,* also exhibit elevated sensitivity when combined with *CSM2* disruption. Upon MMS exposure, deletion of the *APN1* and *APN2* nucleases results in accumulation of AP sites, 3′-dRPs and gapped ssDNA (Figure 3A). Interestingly, *APN1* disruption in a *csm2Δ* cell leads to a synthetic sensitivity upon 0.006–0.012% MMS exposure (Figure 3B). In contrast, *csm2Δ apn2Δ* cells exhibit a very modest synthetic sensitivity at 0.02% MMS (Figure 3C). Since both *apn1Δ* and *apn2Δ* act independently to process abasic sites, their combined

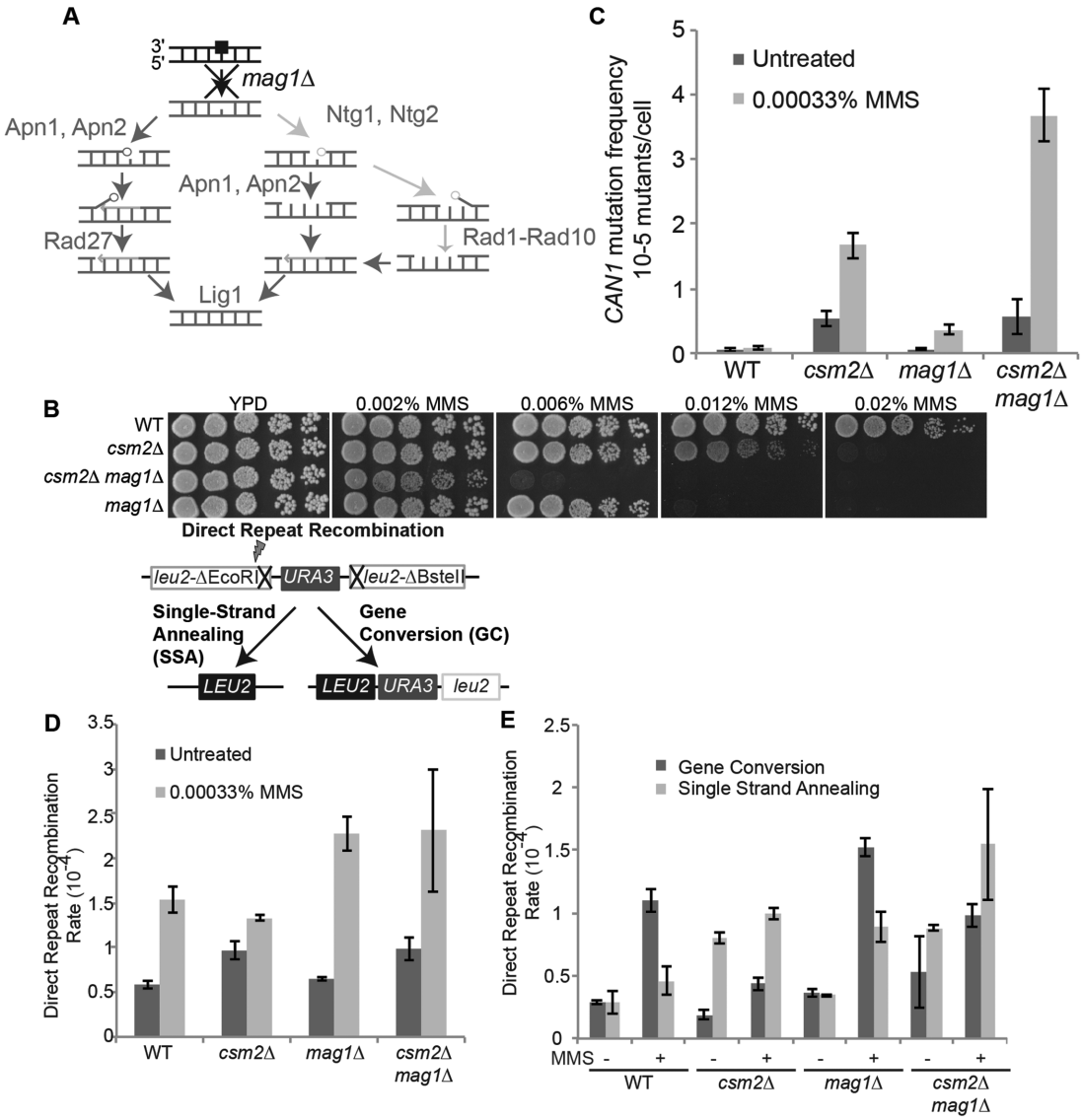

Figure 2. In the absence of the DNA glycosylase *MAG1*, Shu complex disrupted cells are hypersensitive to MMS-induced alkylation damage. (**A**) Cartoon demonstrating what DNA processing step is blocked by *mag1Δ* disruption. (**B**) The indicated yeast strains were 5-fold serially diluted onto YPD medium or YPD medium containing MMS (0.002%, 0.006%, 0.012% and 0.02%) and incubated for two days at 30°C and subsequently photographed. (**C**) Mutation frequencies of WT, *csm2Δ, mag1Δ* and *csm2Δ mag1Δ* cells were determined at the *CAN1* locus both spontaneously and upon MMS exposure. Three experiments with five separate isolates were analyzed and averaged. The graph represents the average of the medians with standard deviations plotted. Significance was determined by t-test. (**D**) Schematic of a direct-repeat recombination assay, where Rad51-dependent gene conversion (GC; *URA3+ LEU2+*) and Rad51-independent single-strand annealing (SSA; *URA3- LEU2+*) repair can be measured. Total recombination rates of the indicated strains are shown before and after MMS treatment. (**E**) The levels of Rad51-dependent (GC) and Rad51-independent (SSA) repair for each condition shown in (D). For (D) and (E), each condition was repeated 3 to 5 times and the average recombination rates were calculated as described in the methods section, are graphed.

deletion creates a stronger MMS sensitivity (33), which we also observe (Figure 3D). When *CSM2* is deleted in *apn1Δ apn2Δ* cells there is a further increase in sensitivity, with cells unable to survive at 0.002% MMS (Figure 3D). Importantly, we find that *MAG1* is epistatic to *APN1* and *APN2* since *csm2Δ mag1Δ* cells exhibit the same growth as a *csm2Δ mag1Δ apn1Δ apn2Δ* quadruple mutant at 0.002% MMS (Figure 3D). These results are consistent with Mag1 functioning upstream to Apn1 and Apn2 (33). Furthermore, we find that not only are *csm2Δ apn1Δ apn2Δ* cells more sensitive to MMS damage but they also exhibit increased spontaneous mutation frequencies (Table 1; $P \leq 0.0007$ comparing *csm2Δ* to *csm2Δ apn1Δ apn2Δ*). Due to the severe MMS sensitivity of *apn1Δ apn2Δ csm2Δ* cells, we are unable to analyze mutation frequencies upon MMS exposure. These results suggest that accumulation of AP sites, 3′-dRPs and/or ssDNA gaps that occur in *apn1Δ apn2Δ* cells are both toxic and mutagenic in the absence of the Shu complex, thereby increasing the hypermutable effects of the ssDNA that is formed (28,38,51,52).

We performed fluorescent microscopy to analyze Rfa1-CFP and Rad52-YFP expressing cells for focus formation

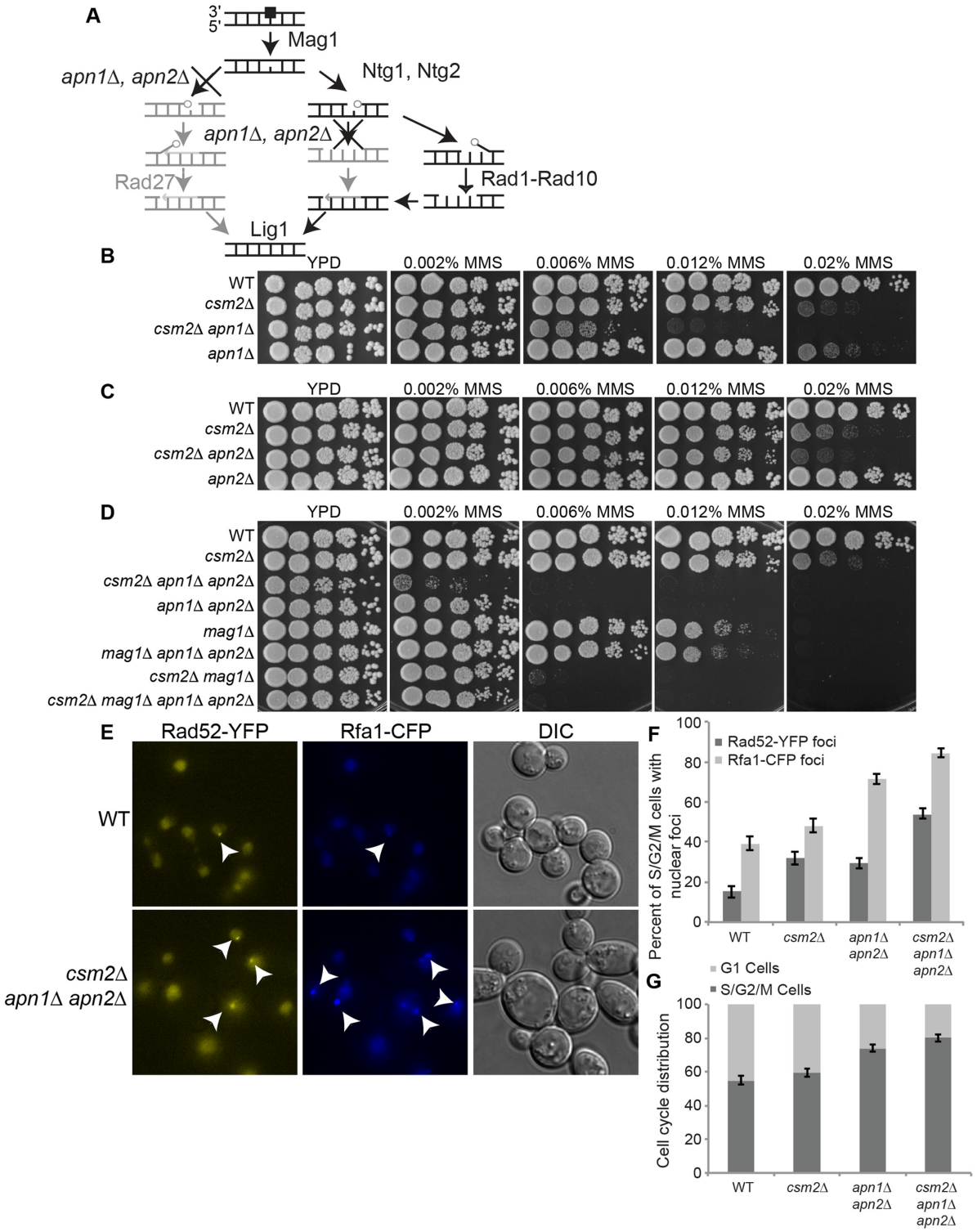

Figure 3. *CSM2* disrupted cells are sensitive to AP sites and/or 3′-dRPs as demonstrated by the synthetic sensitivity of *csm2Δ* with *apn1Δ apn2Δ* on MMS containing medium. (**A**) Cartoon demonstrating what DNA processing steps are blocked by *apn1Δ, apn2Δ* disruption and accumulation of AP sites and 3′-dRPs. (**B** and **C**) The indicated yeast strains were 5-fold serially diluted onto rich medium (YPD) or YPD medium containing the indicated dose of MMS. The plates were incubated at 30°C for two days and photographed. (**D**) In *CSM2* disrupted cells, Mag1 is epistatic to Apn1 and Apn2. The indicated yeast strains were 5-fold serially diluted onto YPD or YPD with MMS as described for (B and C). (**E**) WT, *apn1Δ apn2Δ, csm2Δ* and *apn1Δ apn2Δ csm2Δ* cells expressing Rad52-YFP and Rfa1-CFP were analyzed by fluorescent microscopy for Rad52 and Rfa1 focus formation (indicated by a white arrow). A single z-plane is shown for WT and *apn1Δ apn2Δ csm2Δ* cells. (**F**) The percentage of WT, *apn1Δ apn2Δ, csm2Δ* and *apn1Δ apn2Δ csm2Δ* S/G2/M cells exhibiting a spontaneous nuclear Rad52-YFP or Rfa1-CFP focus. Three individual experiments totaling 300–400 cells were analyzed per genotype and standard error of the means plotted. (**G**) The cell cycle distribution of the indicated genotypes in (E) were measured as a percentage of G1 cells (unbudded) and S/G2/M cells (budded) from the images acquired in (E).

Table 1. Spontaneous mutation frequencies of the indicated strains were determined at the *CAN1* locus

Genotype	Frequency (Mutations/Cell)	Fold Change
WT	2.97×10^{-7}	1
ntg1Δ ntg2Δ	4.01×10^{-7}	1.4
apn1Δ apn2Δ	3.02×10^{-6}	10.2
csm2Δ	4.05×10^{-6}	13.6
csm2Δ ntg1Δ ntg2Δ	3.62×10^{-6}	12.2
csm2Δ apn1Δ apn2Δ	3.72×10^{-5}	125.4
ntg1Δ ntg2Δ apn1Δ apn2Δ	3.2×10^{-5}	108
csm2Δ ntg1Δ ntg2Δ apn1Δ apn2Δ	3.19×10^{-4}	1074.6

indicative of increased ssDNA and HR, respectively, in untreated WT, *apn1Δ apn2Δ* and *csm2Δapn1Δ apn2Δ* cells, as loss of *APN1* and *APN2* results in elevated ssDNA and recombination (28,38,51,52). Indeed, we find Rad52-YFP and Rfa1-CFP foci are significantly elevated in untreated *apn1Δ apn2Δ* budded-cells (indicative of S/G2/M phase) compared to WT (Figure 3E and F, *P*-value < 0.05). Additionally, further deletion of *CSM2* in *apn1Δ apn2Δ* cells results in a significant increase in both Rfa1 and Rad52 foci (Figure 3E and F, *P*-value < 0.05). These results are consistent with slower resolution of Rad52 focus formation occurring in MMS-treated *shu1Δ* cells (19). Furthermore, since we observed an increase in the percentage of budded cells in untreated *csm2Δ apn1Δ apn2Δ*, the slow growth phenotype of this mutant (Figure 3D, YPD plate) may be due to a further accumulation of S/G2/M phase cells than observed in an *apn1Δ apn2Δ* double mutant (Figure 3G, *P*-value $<$ 0.05).

In cells lacking *APN1* and *APN2*, repair of MMS-induced damage during G2 occurs normally in the absence of the Shu complex

Shu complex proteins Csm2 and Psy3 preferentially bind to forked DNA intermediates (20) and its disruption leads to sensitivity to replicative stress, such as that induced by MMS (Figure 1), suggesting that the Shu complex predominately functions in repair and/or tolerance of replicative damage. One possibility is that the Shu complex primarily functions during S phase and, therefore, may be cell cycle regulated. To determine if the Shu complex protein Csm2 is cell cycle regulated, we used alpha factor to arrest Csm2-6HA tagged cells in G1 and then monitored Csm2 protein levels every 20 min after removal of alpha factor. Unlike the G2 cyclin, Clb2, Csm2 protein levels remained relatively constant throughout the time course (Figure 4A). Therefore, Csm2 protein levels are not cell cycle regulated. Similarly, Shu2 and Psy3 protein levels remain constant throughout the cell cycle (Supplementary Figure S3). However, we cannot rule out the possibility that the Shu complex's activity could be regulated by post-translational modification or levels of Shu1, which we have been unable to tag.

To determine if Csm2 may have a role in the repair of MMS-induced DNA lesions during the G2/M cell cycle phase, we analyzed cells for chromosome restitution by pulse-field gel electrophoresis. First, we used nocodazole to arrest WT, *apn1Δ apn2Δ* or *csm2Δapn1Δ apn2Δ* cells in G2 ('C' in Figure 4B). The arrested cells were then treated with 0.1% MMS for 15 min, leading to global chromosomal changes in *apn1Δ apn2Δ* cells due to the accumulation of gapped ssDNA, where T = 0 is taken directly after washing away the MMS (Figure 4B; (38)). The chromosomal changes are revealed as loss of discrete chromosomal bands and the appearance of slow moving DNA (SMD), which is thought to represent chromosomal DNA with excess ssDNA generated during repair (38,51). Chromosome restitution is evident by 8 h following MMS exposure (Figure 4B; compare WT and *apn1Δ apn2Δ* and results in (38,51)). In contrast to previous work showing that chromosome restitution depends on Rad52 and Rad51 (38), we find that the faint chromosome restitution visible in *apn1Δ apn2Δ* cells occurs independently of Csm2 during G2 across multiple trials (Figure 4B).

We next asked if the Shu complex would be required for the bypass of MMS-induced lesions during S-phase. WT and *csm2Δ* cells were arrested in G1 with alpha factor. Cells were released from alpha factor for 10 min before being treated with 0.033% MMS for 1 h (45). As cells progress into S-phase, their chromosomes are unable to be visualized by PFGE (Figure 4C, T = 0) due to accumulation in the well, but upon entry into G2, their chromosomes become visible (45). In WT cells, chromosome restitution can be visualized by 60 min (Figure 4C). In contrast, chromosome restitution in *csm2Δ* cells is delayed to ∼4 h (Figure 4C). These results are consistent with cell cycle profiles of an MMS-treated *PSY3* mutant (22). These results indicate that while the Shu complex is present throughout the cell cycle, it functions predominately during S phase to bypass MMS-induced damage and has no significant contribution to the repair of similar lesions in G2 cells.

NTG1 and *NTG2* generate toxic BER intermediates in the absence of *APN1* and *APN2*

To determine if the Shu complex is responding to both abasic sites and ssDNA breaks in *apn1Δ apn2Δ* cells, we also deleted *NTG1* and *NTG2* to block the formation of ssDNA breaks (Figure 3A). Ntg1 and Ntg2 are bifunctional DNA glycosylases with associated apurinic/apyrimidinic (AP) lyase activities that cleave abasic sites to generate 3′-dRPs and their disruption results in AP sites being primarily processed by Apn1 and Apn2 (Supplementary Figure S2A). We sought to determine how the Shu complex responds to abasic sites, using various combinations of mutants. In contrast to *csm2Δ mag1Δ* or *csm2Δ apn1Δ apn2Δ*, we do not observe an elevated sensitivity in *csm2Δ ntg1Δ* (Supplementary Figure S2B), *csm2Δ ntg2Δ* (Supplementary Figure S2C) or *csm2Δ ntg1Δ ntg2Δ* cells upon MMS

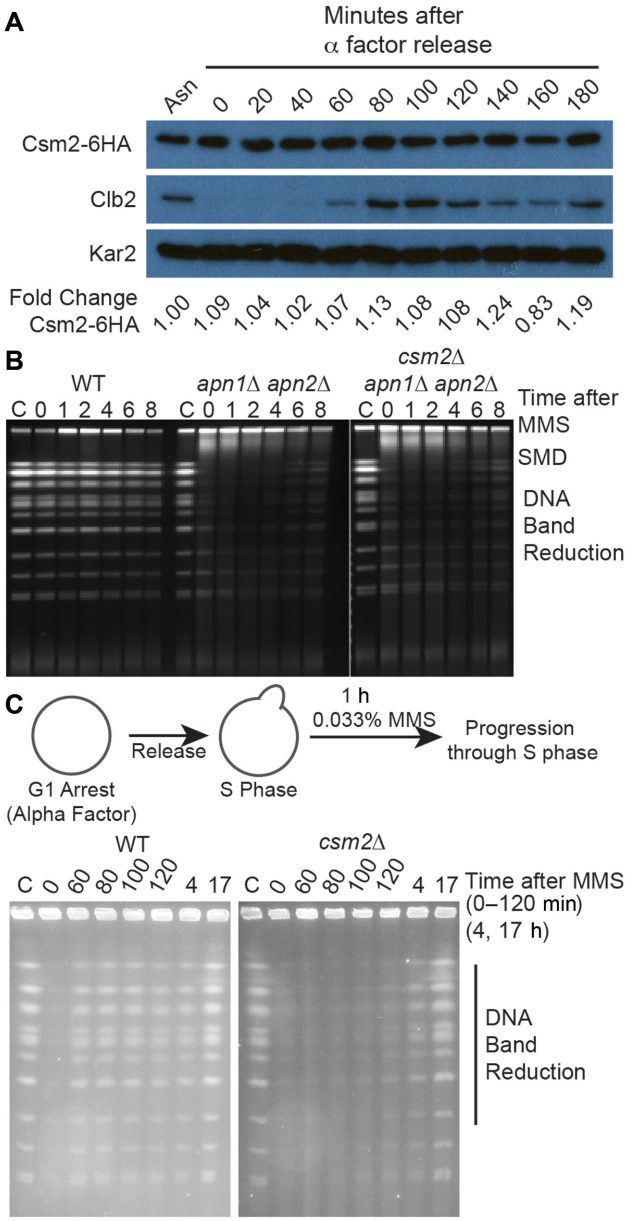

Figure 4. *CSM2* is important for repair of MMS-induced damage during S phase but not G2 phase. (**A**) Protein levels of Csm2, Clb2 (S/G2-phase control) and Kar2 (loading control) in asynchronous (ASN) cells or after release from G1 arrest by alpha factor. (**B**) Chromosome shattering and restitution in WT, *apn1Δ apn2Δ* and *apn1Δ apn2Δ csm2Δ* cells arrested in G2 cell cycle by nocodazole. Chromosomes are harvested at the indicated time points before and after treatment with MMS and separated by PFGE as described in the methods. (**C**) Chromosome restitution following progression through S phase in WT or *csm2Δ* cells treated with MMS.

exposure (Supplementary Figure S2D). Nor do we observe an increase in spontaneous mutation frequencies in *csm2Δ ntg1Δ ntg2Δ* cells (Table 1; $P \geq 0.5$ comparing *csm2Δ* to *csm2Δ ntg1Δ ntg2Δ*). Furthermore, we find that *MAG1* is epistatic to *NTG1* and *NTG2* where a *csm2Δ mag1Δ* exhibits the same defect as a *csm2Δ mag1Δ ntg1Δ ntg2Δ* cell (Supplementary Figure S2D).

In the absence of *APN1* and *APN2*, Ntg1 and Ntg2 cleave abasic sites to generate 3′-dRPs, which can be converted into toxic one-ended DSBs upon replication (Figure 5A) (35). Consistently, we observe a synthetic rescue of the MMS sensitivity of an *apn1Δ apn2Δ* double mutant in *apn1Δ apn2Δ ntg1Δ ntg2Δ* cells at 0.006% MMS (Figure 5B) (38). Interestingly, *csm2Δ apn1Δ apn2Δ ntg1Δ ntg2Δ* cells also grow better than *csm2Δ apn1Δ apn2Δ* cells at 0.002% MMS (Figure 5B), indicating that the Shu complex may act on abasic sites as well as one-ended DSBs that could be generated by replication forks encountering a ssDNA break. Quite surprisingly, although deletion of *NTG1* and *NTG2* suppresses the severe MMS sensitivity of *apn1Δ apn2Δ* cells by removing the toxic ssDNA breaks formed, we find that the spontaneous mutation frequency of *apn1Δ apn2Δ ntg1Δ ntg2Δ* cells is approximately 10-fold higher than *apn1Δ apn2Δ* cells (Table 1). These unexpected results suggest that the high mutation frequency caused by abasic sites is significantly less toxic than formation of ssDNA breaks. Furthermore, we find that disruption of *CSM2* in *apn1Δ apn2Δ ntg1Δ ntg2Δ* cells can further increase the spontaneous mutation frequency over 1000-fold compared to WT, underscoring a novel and important new role for the Shu complex in the error-free bypass of abasic sites (Table 1). Consistent with these results, increased spontaneous mutation frequencies are also observed in *ntg1Δ ntg2Δ apn1Δ rad52Δ* cells (150-fold; (53)). To determine if the abasic sites are bypassed by Shu complex dependent HR, we measured the rate of spontaneous recombination using the direct repeat recombination assay described above (Figure 2D). In agreement with our finding that *apn1Δ apn2Δ* cells exhibit elevated Rad52 foci and slow growth in combination with *csm2Δ* (Figure 3F and D, respectively), we find a nearly 10-fold increased recombination rate in *apn1Δ apn2Δ* cells compared to WT (Figure 5B and C, P-value < 0.001). Over half the recombination increase relies upon *CSM2* based on the 50% reduction in *csm2Δapn1Δ apn2Δ* cells (Figure 5B, P-value < 0.005). Similarly, the elevated recombination of *apn1Δ apn2Δ ntg1Δ ntg2Δ* cells is suppressed by *csm2Δ* (Figure 5B, P-value < 0.01). Surprisingly, while deletion of *NTG1* and *NTG2* promotes increased MMS resistance of *apn1Δ apn2Δ* cells, we find that deletion of *NTG1* and *NTG2* do not rescue the elevated recombination rates of *apn1Δ apn2Δ* cells. Unfortunately, fluorescently tagged Rad52 and Rfa1 in *apn1Δ apn2Δ ntg1Δ ntg2Δ* and *csm2Δ apn1Δ apn2Δ ntg1Δ ntg2Δ* cells resulted in extremely poor growth and lethality, respectively. Therefore, we were unable to measure the levels of Rad52 and Rfa1 foci in these cells.

Next, we measured mutation frequencies in *apn1Δ apn2Δ* and *apn1Δ apn2Δ ntg1Δ ntg2Δ* cells in the presence or absence of *CSM2*. Deletion of *CSM2* resulted in an approximate 10-fold increase in mutation frequencies (Table 1), indicating that the majority of spontaneous lesions are preferentially bypassed by high-fidelity rather than error-prone mechanisms. As expected, the reduced recombination rate resulting from *CSM2* deletion is due to a decrease in Rad51-dependent gene conversion while Rad51-independent SSA remains constant (Figure 5D). While a *csm2Δ* cell exhibits a significant increase in Rad51-independent SSA (20)(Figure 5D, P-value < 0.001), we do not observe an increase in SSA if *CSM2* is disrupted in *apn1Δ apn2Δ* or *apn1Δ apn2Δ*

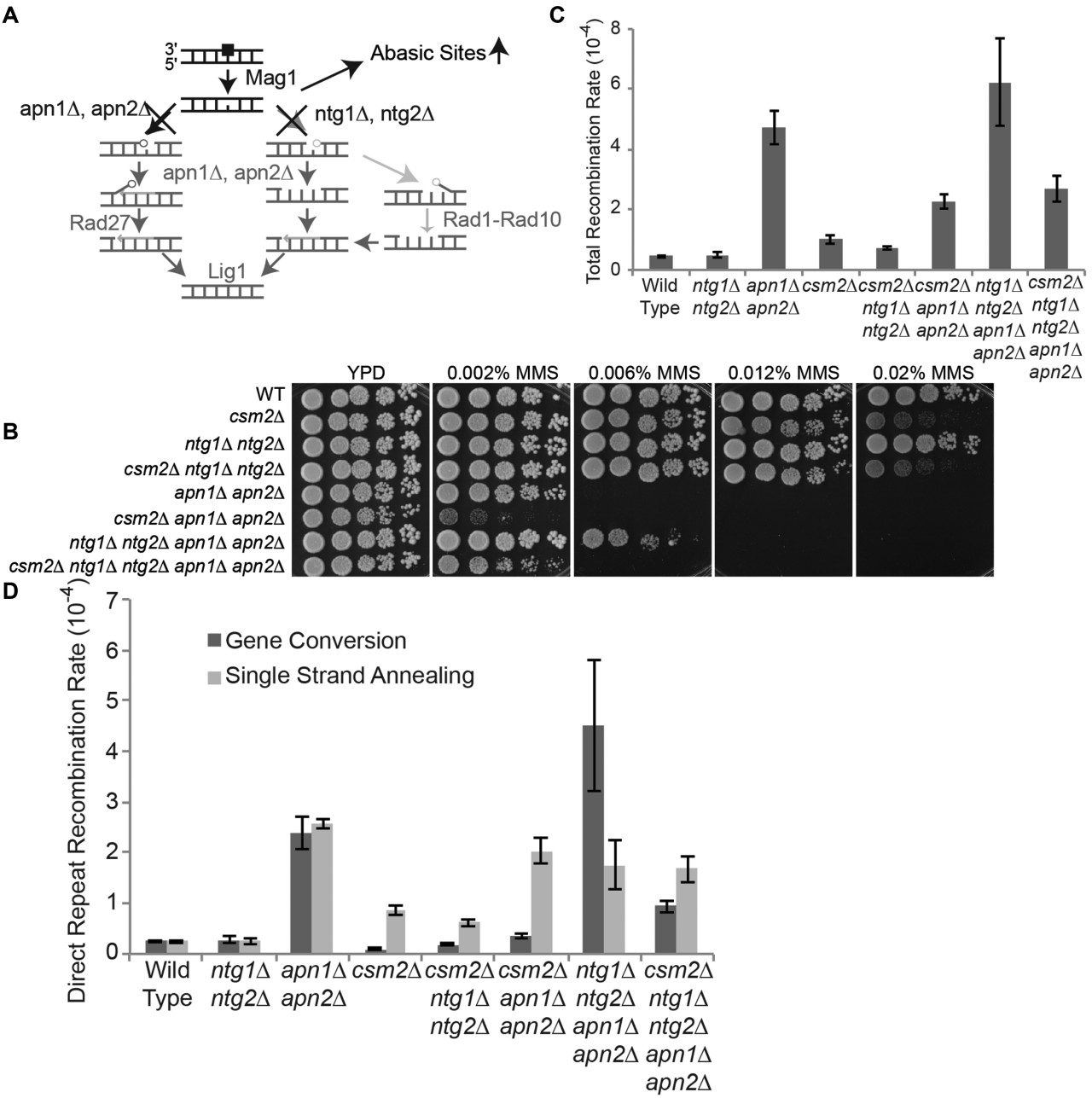

Figure 5. *CSM2* disrupted cells are sensitive to AP sites as demonstrated by the synthetic sensitivity of *csm2Δ* with *apn1Δ apn2Δ ntg1Δ ntg2Δ* on MMS containing medium. (**A**) Cartoon demonstrating what DNA processing steps are blocked by *apn1Δ, apn2Δ, ntg1Δ* and *ntg2Δ* disruption and accumulation of AP sites. (**B**) The indicated yeast strains were 5-fold serially diluted onto rich medium (YPD) or YPD medium containing the indicated dose of MMS. The plates were incubated at 30°C for two days and photographed. (**C**) The total recombination rates, as in Figure 2D. (**D**) The levels of Rad51-dependent and independent repair as in Figure 2E.

ntg1Δ ntg2Δ cells (Figure 5D). Perhaps, cells are unable to perform SSA or an SSA-like event in a replicative context (50).

While *apn1Δ apn2Δ* and *apn1Δ apn2Δ ntg1Δ ntg2Δ* cells exhibit similar overall levels of recombination rates, the distribution of GC and SSA-like events differs significantly. For example, the spontaneous recombination events caused by abasic sites in an *apn1Δ apn2Δ ntg1Δ ntg2Δ* strain are significantly biased toward Rad51-dependent repair similar to MMS treated WT or *mag1Δ* cells (compare Figures 2E and 5D), whereas the spontaneous recombination events caused by the abasic sites and ssDNA breaks in *apn1Δ apn2Δ* cells give rise to equivalent levels of Rad51-dependent and -independent repair, similar to untreated WT cells but at ∼10-fold higher rates (Figure 5D). The different recombination outcomes observed in *apn1Δ apn2Δ* and *apn1Δ apn2Δ ntg1Δ ntg2Δ* cells indicate that the distinct lesions that accumulate in these cells result in divergent HR outcomes. Since it has been shown that there may be more 3′-dRPs and fewer abasic sites in *apn1Δ apn2Δ* cells,

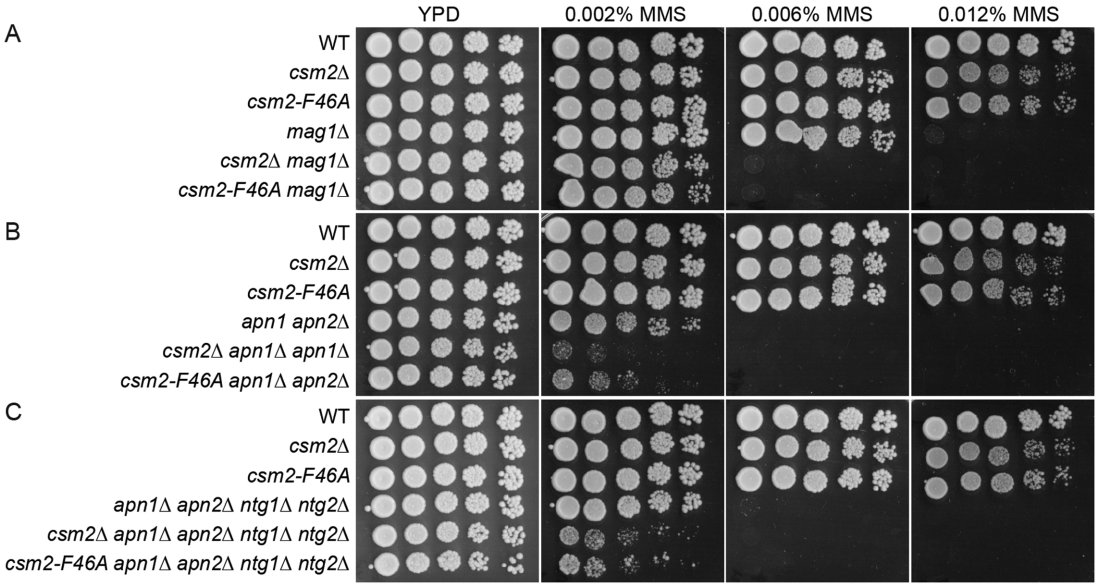

Figure 6. Cells containing *csm2-F46A* are defective for tolerance of BER lesions. (**A**–**C**) The indicated yeast strains were 5-fold serially diluted onto rich medium (YPD) or YPD medium containing the indicated doses of MMS.

as Ntg1 and Ntg2 can directly process abasic sites into 3′-dRPs, our data indicate that abasic sites preferentially activate Rad51-dependent recombination while 3′-dRPs trigger a higher percentage of Rad51-independent recombination (35). Importantly, the strong bias toward Rad51-dependent GC that we observe here suggest that the primary recombinogenic lesion in MMS treated cells with functional BER is likely to be an N3-MeA or an abasic site rather than an ssDNA break that encounters a replication fork. Critically, in each case observed, the Shu complex is essential to ensure this bias toward Rad51-dependent HR.

Csm2 physical interaction with Rad55 is essential for promoting repair of N3-MeAs and abasic sites

Recently, we uncovered that a single point mutation in Csm2, csm2-F46A, abrogates Csm2's physical interaction with Rad55, resulting in impaired Rad51 filament formation (10). To determine if the ability of the Shu complex to associate with Rad55 is important for promoting tolerance to different MMS-induced lesions, we compared the MMS sensitivities of *mag1Δ, apn1Δ apn2Δ* and *apn1Δ apn2Δ ntg1Δ ntg2Δ* cells (Figure 6) with cells that are also *csm2Δ* or *csm2-F46A* mutants. Like *csm2Δ* cells, we observe similar DNA damage sensitivities when a *csm2-F46A* mutant is combined with *mag1Δ* (Figure 6A), *apn1Δ apn2Δ* (Figure 6B) or *apn1Δ apn2Δ ntg1Δ ntg2Δ* (Figure 6C). Note that *csm2-F46A apn1Δ apn2Δ* cells are less MMS sensitive than *csm2Δ apn1Δ apn2Δ* cells (Figure 6B). Perhaps the residual interaction between csm2-F46A and Rad55 (<5% of WT, (10)) is sufficient to promote limited repair in this context. Together, these data demonstrate that the ability of the Shu complex to associate with Rad55 is essential to promote cell viability in response to each BER lesion examined.

The *csm2Δ rad27Δ* growth defect is complemented by human Polβ

To further investigate the role of the Shu complex in repairing ssDNA breaks, we also evaluated the impact of Rad27 on repair of MMS associated breaks. Rad27/FEN1 is a flap endonuclease, which is important for Okazaki fragment processing as well as excising the 5′-dRPs created by Apn1 and Apn2 (Figure 7A). To examine if the Shu complex repairs ssDNA breaks generated in a *rad27Δ* cell similar to those generated by *apn1Δ apn2Δ*, we compared the growth of WT, *csm2Δ*, *rad27Δ* and *csm2Δ rad27Δ* cells in the presence or absence of MMS (Figure 7B). The double *csm2Δ rad27Δ* mutant cells exhibit a slow growth phenotype that is exacerbated upon MMS exposure (Figure 7B). The survival in response to 0.006% MMS is decreased in *csm2Δ rad27Δ* compared to *rad27Δ*. Interestingly, the MMS sensitivity of *rad27Δ* cells is not rescued by deletion of *MAG1* as would be expected if Mag1 functioned upstream of Rad27 (Figure 7B), indicating that the MMS sensitivity of a *rad27* mutant may not solely reflect a defect in the BER pathway. In agreement with this observation, the slow growth of *csm2Δ rad27Δ* is not rescued by *MAG1* deletion (0.002% MMS; Figure 7B).

It was recently shown that expression of human Polβ partially complements the MMS sensitivity of *rad27Δ* cells (54). We confirmed this observation by expressing human Polβ under a GAL or GPD promoter on a CEN plasmid (Figures 6E and 7C). In contrast to *rad27Δ* cells, expression of human Polβ does not suppress the MMS sensitivity of Shu complex mutants (Figure 7D), indicating that accumulation of 5′ dRPs is not the primary cause of toxicity in MMS-treated *csm2Δ* cells. However, human Polβ does rescue the slow growth of a *csm2Δ rad27Δ* double mutant as well as its MMS sensitivity at 0.002% MMS (Figure 7E). The observation that overexpression of Polβ, but not deletion of *MAG1,* suppresses the MMS sensitiv-

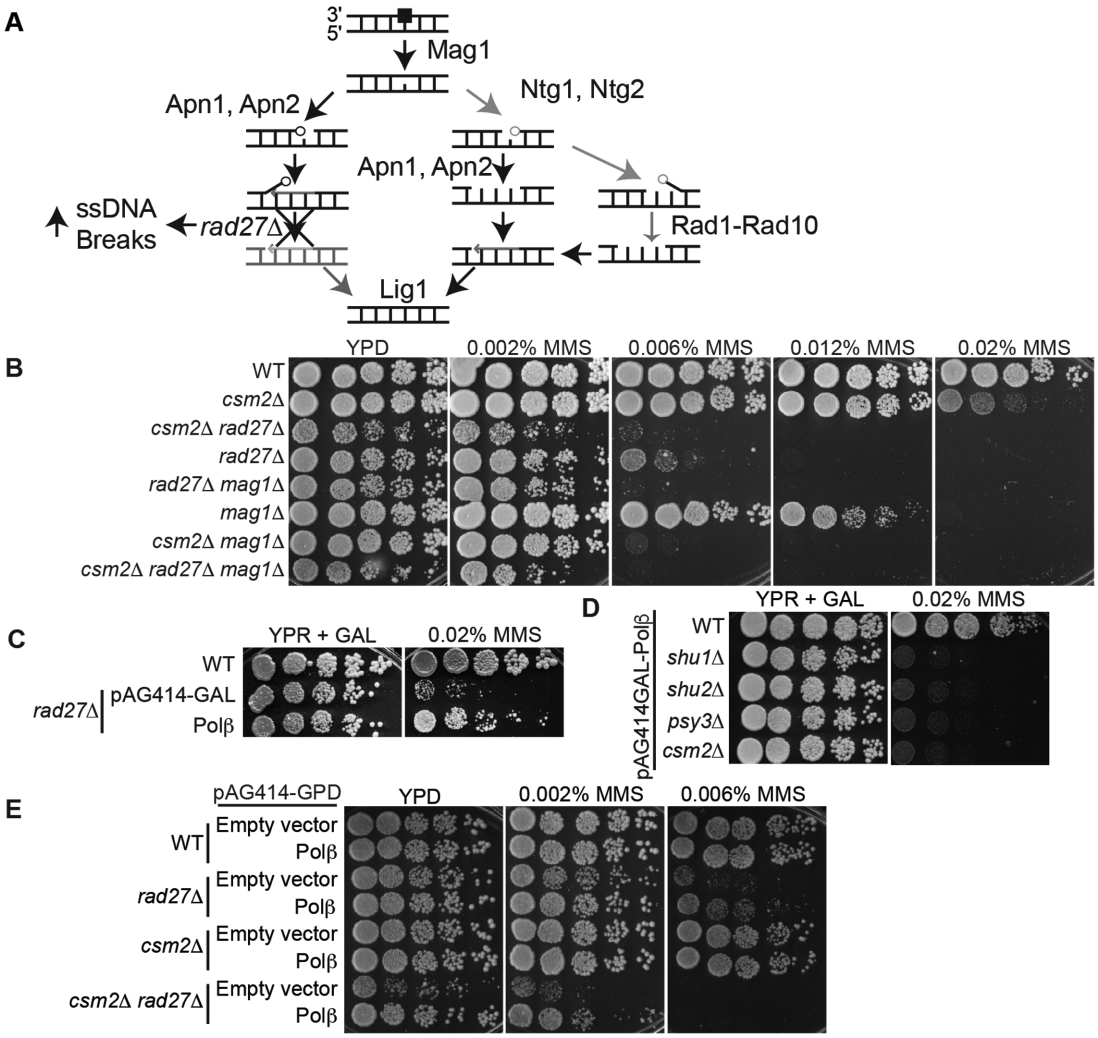

Figure 7. Expression of human Polβ partially suppresses the MMS sensitivity of *rad27Δ* cells and the synthetic growth defect observed in *csm2Δrad27Δ* double mutant cells. (**A**) Cartoon indicating what processing step is blocked by *rad27Δ* disruption. (**B**) The indicated yeast strains were 5-fold serially diluted onto YPD medium or YPD medium containing 0.002%, 0.006%, 0.012% or 0.02% MMS where indicated. The plates were incubated at 30°C for two days and photographed. (**C**) WT cells or *rad27Δ* cells which also express either an empty vector (pAG414-GAL) or the human Polβ in an expression plasmid (pAG414-GAL-Polβ) were 5-fold serially diluted and plated onto YPRaffinose with galactose (YPR + GAL) medium or YPR + GAL medium containing 0.02% MMS. The cells were incubated at 30°C for two days and photographed. (**D**) WT, *shu1Δ, shu2Δ, psy3Δ, csm2Δ* cells were transformed with pAG414-GAL-Polβ, 5-fold serially diluted and plated onto YPR + GAL medium or YPR + GAL medium containing 0.02% MMS. The plates were incubated at 30°C for two days and photographed. (**E**) WT, *rad27Δ, csm2Δ, csm2Δ rad27Δ* cells were transformed with either the pAG414-GPD (Empty Vector) or the pAG414-GPD-Polβ (Polβ) plasmid and 5-fold serially diluted onto YPD or YPD medium containing 0.002% or 0.006% MMS. The plates were incubated at 30°C for two days and photographed.

ity of a *rad27Δ* suggests that *rad27Δ* cells are not necessarily sensitive to MMS due to the lesions produced by Mag1-dependent repair of methylated DNA. One possibility may be that spontaneous loss of MMS-induced base lesions, such as N7-MeG, contributes to the sensitivity that is suppressed by overexpression of Polβ. Although it is more likely that the incomplete rescue of *rad27Δ* by *mag1Δ* suggest additional repair mechanisms, independent of BER, underlie the MMS sensitivity of *rad27Δ* cells. Perhaps the slowed replication fork progression in MMS-treated cells generates shorter, more frequent Okazaki fragments, which are normally processed by Rad27.

Translesion synthesis is required for bypassing MMS-induced DNA damage in *csm2Δ apn1Δ apn2Δ* and *csm2Δ mag1Δ* cells

Disruption of the Shu complex leads to increased mutation frequencies, which depends on *REV7*/*REV3*, the DNA translesion polymerase zeta (Polζ) (19,22). To determine if Pol ζ is required to bypass the DNA damage intermediates that accumulate in *csm2Δ, csm2Δ apn1Δ apn2Δ* or *csm2Δ mag1Δ* cells, we examined the MMS sensitivity of different mutant combinations in the presence or absence of *REV3*, the catalytic subunit of polymerase ζ. The *csm2Δ rev3Δ* double mutants exhibit synthetic sensitivity upon exposure to 0.006% MMS, similar to *psy3Δ rev3Δ* cells (Figure 8A; (22)). We find that the synthetic lethal-

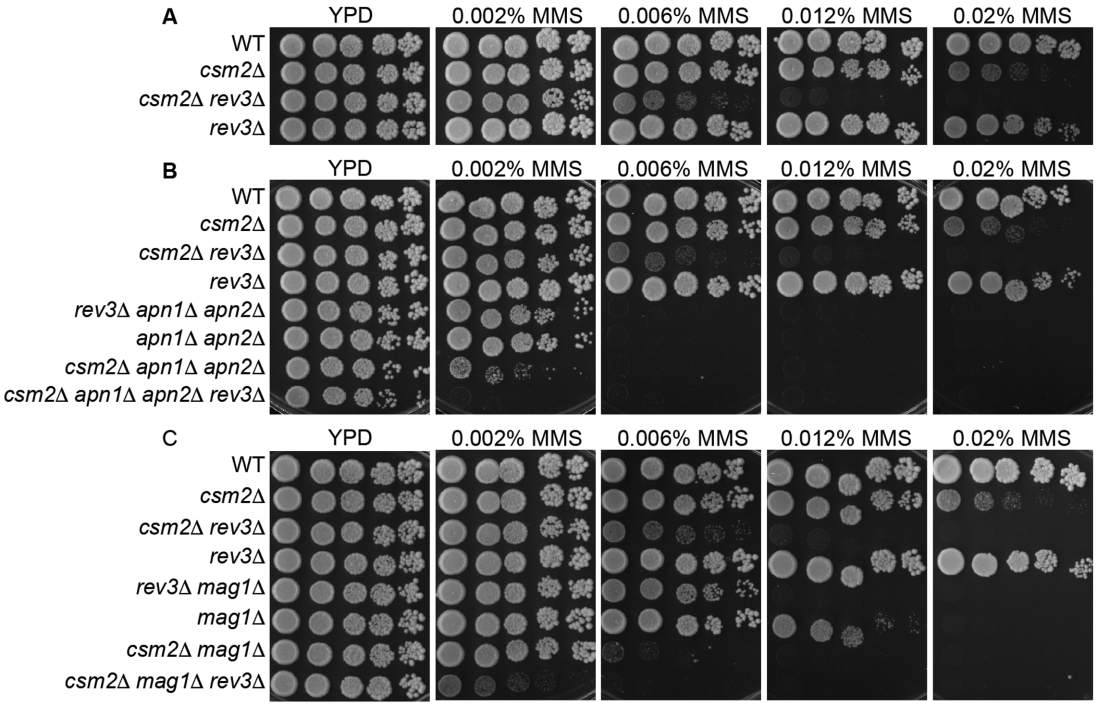

Figure 8. The translesion DNA polymerase ζ is necessary for lesion bypass in MMS-exposed *csm2Δ apn1Δ apn2Δ* or *csm2Δ mag1Δ* cells. (**A**–**C**) The indicated genotypes were 5-fold serially diluted onto YPD medium or YPD medium containing 0.002%, 0.006%, 0.012% or 0.02% MMS. The plates were incubated at 30°C for two days and photographed.

ity in MMS-exposed *csm2Δ rev3Δ* cells is further exacerbated by deletion of *APN1* and *APN2* (*csm2Δ apn1Δ apn2Δ rev3Δ* 0.002% MMS; Figure 8B) or *MAG1* disruption (*csm2Δ mag1Δ rev3Δ* 0.002% MMS; Figure 8C). Interestingly, while *mag1Δ* and *rev3Δ* are synthetic sensitive (Figure 8C), *apn1Δ apn2Δ* and *rev3Δ* are not as long as Csm2-associated HR is functional (Figure 8B). These results suggest that abasic sites are preferentially bypassed by error-free post-replicative repair and TLS is only initiated if HR is impaired.

Epistasis analysis of *csm2Δ* and the error-free post-replicative repair genes *rad5Δ, ubc13Δ, mms2Δ*

Since we find that TLS likely bypasses the lesions created in the absence of *CSM2*, one possibility is that the Shu complex functions in the error-free branch of the post-replicative repair (PRR) pathway. To address this possibility, we combined *csm2Δ* with deletion of the three genes involved in initiating error-free PRR (*rad5Δ*, *ubc13Δ* or *mms2Δ*) (Figure 9). We find a slight, but reproducible, synthetic growth defect between *csm2Δ* and disruption of these three genes upon MMS exposure (Figure 9A). The growth effect is small at best at a higher level of MMS. Please note the *rad5Δ* mutants are significantly more sensitive to MMS than either *ubc13Δ* or *mms2Δ* mutants (Figure 9A). A further synthetic effect was observed for spontaneous mutation frequencies and recombination rates. We find that mutation frequencies in the *csm2Δ rad5Δ* and *csm2Δ ubc13Δ* double mutants are elevated compared to the corresponding single mutants (Figure 9B; *P*-value 0.009 and 0.01, respectively). Similarly, we observe decreased rates of GC in these same *csm2Δ rad5Δ* and *csm2Δ ubc13Δ* double mutants relative to their single mutants. However, only *csm2Δ ubc13Δ* is significant value (*P*-value 0.03), whereas *csm2Δ rad5Δ* trended toward significance (Figure 9C). In contrast, we do not observe a significant change in Rad51-independent SSA. Surprisingly, these results suggest that the Shu complex may have functions outside of error-free PRR.

DISCUSSION

MMS-induced DNA damage is repaired through both the BER and HR machineries (29,55). Although the DNA lesions created by MMS are primarily repaired through BER, if the DNA damage occurs during S phase and repair is not complete by the time the replication fork encounters the lesion, then a subset of these DNA repair intermediates can lead to replication fork stalling and collapse (25,38,56,57). Stalled forks may bypass blocking lesions such as N3-MeA through potentially mutagenic translesion DNA polymerases (58). Alternatively, HR can be used to bypass a lesion at a stalled replication fork or to repair a break after a replication fork collapses. The handoff from one repair pathway to another and which DNA intermediates are substrates for the HR machinery is not well understood.

Here, we describe how the Shu complex acts to channel normal BER intermediates into the HR pathway, which also reduces the risk of mutagenesis. The major phenotypes observed in cells disrupted for the Shu complex are an elevated mutation frequency and a heightened sensitivity to the model alkylating agent MMS, which produces replicative blocking lesions such as N3-MeA and N7-MeG (Figure 10)(19,22,24). In cells disrupted for *MAG1*, the primary

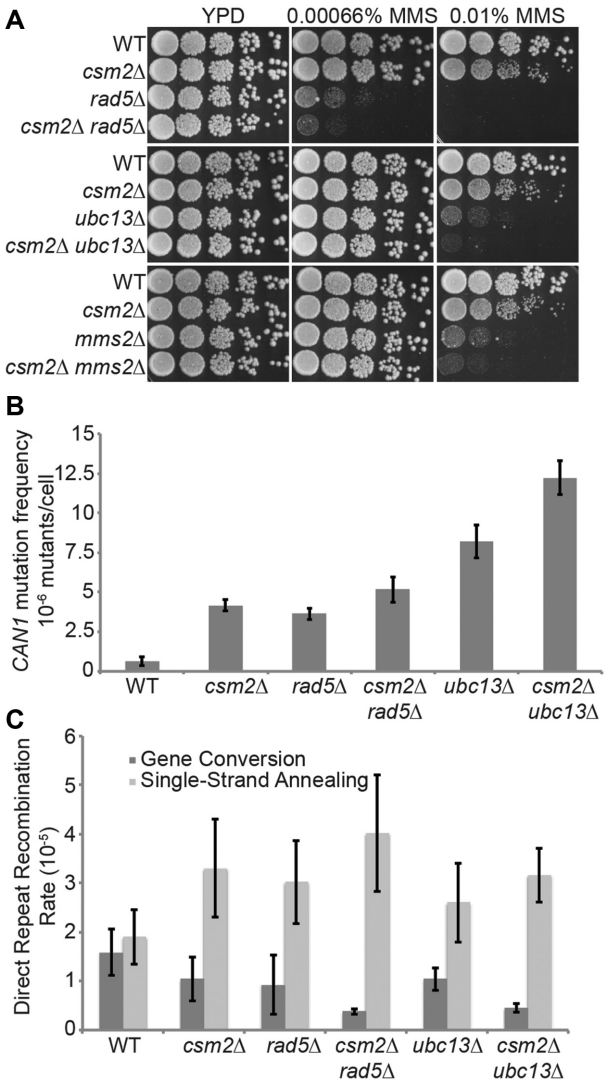

Figure 9. Analysis of *CSM2*-disrupted cells with error-free PRR disruption (*rad5Δ, ubc13Δ, mms2Δ*) by MMS sensitivity, mutation frequencies and direct repeat recombination rates. (**A**) The indicated yeast strains were 5-fold serially diluted onto rich medium (YPD) and YPD medium containing the indicated dose of MMS. The plates were incubated for two days at 30°C and photographed. (**B**) Mutation frequencies were determined in the indicated strains at the *CAN1* locus. Three experiments with five separate isolates were analyzed and averaged. The graph represents the average of the medians with standard deviations plotted. Significance was determined by t-test. (**C**) The rate of gene conversion and SSA-like events were measured as described in Figure 2E. Three to four experiments were done per strain and standard deviations plotted. Significance was determined by t-test.

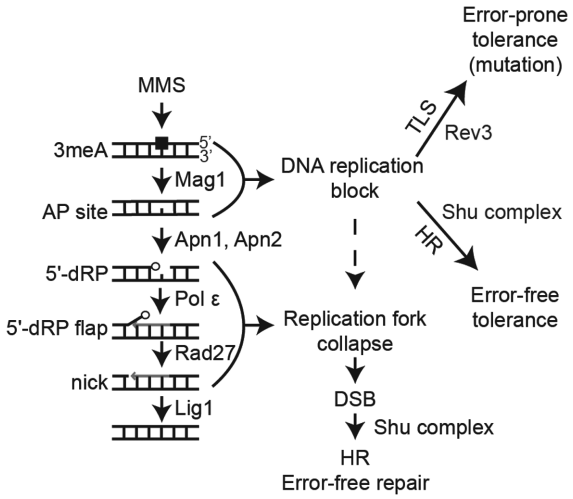

Figure 10. Overview repair model of MMS-induced DNA damage in budding yeast by BER, translesion DNA synthesis (TLS) and HR (Adapted from (55)). MMS damage leads to base lesions excised by the DNA glycosylase Mag1 to create an AP site. Both the MMS-induced base lesions and AP sites can lead to a replication fork block, which can either be bypassed by the TLS pathway (requiring Rev3) resulting in increased mutation frequency and therefore, error-prone repair (69). During BER, Apn1/Apn2 further processes the AP site leading to 5′-dRPs, which are filled in by DNA polymerase ϵ and the 5′-dRP flap is cleaved by Rad27. Lig1 ligates the resulting nick. The 5′-dRP and flap as well as the nicked DNA can lead to replication fork collapse and DSB formation. The resulting DSB can be repaired by the high-fidelity HR pathway via the Shu complex, which is important for the critical Rad51 filament formation step of HR.

glycosylase that recognizes and excises MMS-induced base lesions (31,48,49), loss of the Shu genes causes a synthetic sensitivity to MMS. These results indicate that irreparable ss breaks lead to DSBs, while AP sites or methylated bases lead to ss gaps that are substrates for error-free bypass and the Shu complex (47). Interestingly, disruption of the abasic site endonucleases *APN1* (59) and *APN2* (60) causes an even more pronounced synthetic growth defect when combined with Shu gene disruptions, suggesting that the Shu complex also participates in repair of abasic sites during aborted or interrupted BER. Furthermore, our genetic evidence indicates that the Shu complex also repairs DNA with 3′-dRPs that are produced during BER and are incredibly toxic due to their inability to be acted upon by DNA polymerases (61).

Moving forward, it will be interesting to examine if Ogg1, which can also act on abasic sites to generate ssDNA breaks, will similarly suppress an *apn1Δ apn2Δ csm2Δ* cell resulting in elevated mutagenesis and recombination. Surprisingly, we provide evidence that the Shu complex may have a function outside of the error-free PRR pathway. Finally, disruption of Rad27/FEN1, the flap endonuclease that removes a stretch of nucleotides to allow repair during BER (62), also causes an extreme synthetic sensitivity to MMS when the Shu complex is disrupted. This sensitivity is alleviated when human Polβ is expressed indicating that the Shu complex is required to resolve the numerous ssDNA breaks left when Rad27/FEN1 is missing (54). Taken together, our genetic evidence demonstrates that there is a close crosstalk between the BER and HR repair pathways, where normal repair intermediates produced during BER are repaired and resolved faithfully by HR to minimize mutagenesis during DNA replication.

Despite its role in regulating HR through Rad51 filament formation, loss of the Shu complex creates a more modest phenotype when compared to loss of its binding partners *RAD55* and *RAD57* (10,20). For instance, *rad55Δ* cells are sensitive to a broader range of damaging agents, such as UV and H_2O_2, both of which would cause replication fork stalling base modifications. Why the Shu complex is not sen-

sitive to these agents, while Rad55 mutants are, remains an open question. One hypothesis is that, while Rad55-Rad57 is known to function during S and G2 phase (45,64), it has been suggested that the Shu complex functions primarily during replicative stress in S phase (21,22,24). Here, we directly test the hypothesis that the Shu complex has a role in repair during replicative stress. We find no compelling evidence that the Shu complex functions during G2/M. Although the protein levels of the Shu complex members Shu2, Csm2 and Psy3 remain constant throughout the cell cycle, we find that in G2 arrested cells treated with MMS, chromosome restitution is independent of the Shu complex.

Together, our data suggest a model whereby the Shu complex responds to numerous BER intermediates, including the replicative blocking MMS-induced base lesions such as N3-MeA, the highly mutagenic abasic site, cytotoxic ssDNA breaks and blocked ends that generate a full DSB during replication, all in the specific context of replicative stress. These results may suggest that the lethality of *rad55* mutants in UV or H_2O_2 exposed cells may occur due to DSBs arising from lesions outside of S phase, when the Shu complex is not active. Treatment of cells disrupted for the Shu complex with chronic UV exposure, which increases a cell's reliance on bypass mechanisms, may reveal a previously unknown UV sensitivity in these cells. Alternatively, the lesions produced by UV and H_2O_2 may not be channeled into Shu complex dependent HR, indicating that different replication fork blocking lesions may initiate different forms of HR.

Recent work has clearly demonstrated that numerous human conditions such as cancer predisposition and Fanconi anemia arise from defects in HR proteins such as BRCA1/2, RAD51 and the RAD51 paralogues (65,66). Similarly, aging and cancer have also been attributed to defects in BER (67). It has been shown that cancers with defective HR are exquisitely sensitive to PARP1 inhibitors, which block PARP1 function and increase the amount of ssDNA breaks that give rise to DSBs and require repair by HR (68). Our work in budding yeast creates a framework for understanding and studying the crosstalk between BER intermediates and HR that could have important implications for cancer treatment. For example, our work suggests that there are multiple other targets worth inhibiting for the treatment of cancers with defective HR. Inhibition of human APN1/2 (APE1/2), as well as human Rad27 (FEN1), would likely result in extreme synthetic lethality in such tumors just like PARP1 inhibition. Finally, our work strongly supports the importance of investigations of combinations of PARP1 inhibitors and chemotherapeutic agents. Clinical trials addressing such combinations are currently underway.

SUPPLEMENTARY DATA

Supplementary Data are available at NAR Online.

ACKNOWLEDGEMENTS

The authors thank Susan Lindquist for the pAG414-GPD-ccdB and pAG414-GAL-ccdB plasmids (Addgene plasmids 14144 and 14143, respectively). R.W.S. is an Abraham A. Mitchell Distinguished Investigator at the Mitchell Cancer Institute.

FUNDING

National Institutes of Health (NIH) [GM088413, ES024872 to K.A.B. and CA148629, GM087798 to R.W.S.]; V Foundation Scholar Award (to K.A.B.); China Scholarship Council to (Z.Z.); Intramural Research Program of the National Institute of Environmental Health Sciences, NIH [project 1 Z01 ES065073 to M.A.R.]. Funding for open access charge: NIH [ES024872 to K.A.B].

Conflict of interest statement. R.W.S. is a scientific consultant for Trevigen, Inc.

REFERENCES

1. Mathiasen,D.P. and Lisby,M. (2014) Cell cycle regulation of homologous recombination in *Saccharomyces cerevisiae*. *FEMS Microbiol. Rev.*, **38**, 172–184.
2. Agmon,N., Liefshitz,B., Zimmer,C., Fabre,E. and Kupiec,M. (2013) Effect of nuclear architecture on the efficiency of double-strand break repair. *Nat. Cell Biol.*, **15**, 694–699.
3. Mine-Hattab,J. and Rothstein,R. (2013) DNA in motion during double-strand break repair. *Trends Cell Biol.*, **23**, 529–536.
4. Jasin,M. and Rothstein,R. (2013) Repair of strand breaks by homologous recombination. *Cold Spring Harb. Perspect. Biol.*, **5**, a012740.
5. Burgess,R.C., Lisby,M., Altmannova,V., Krejci,L., Sung,P. and Rothstein,R. (2009) Localization of recombination proteins and Srs2 reveals anti-recombinase function in vivo. *J. Cell Biol.*, **185**, 969–981.
6. Karpenshif,Y. and Bernstein,K.A. (2012) From yeast to mammals: Recent advances in genetic control of homologous recombination. *DNA Repair (Amst)*, **11**, 781–788.
7. Holthausen,J.T., Wyman,C. and Kanaar,R. (2010) Regulation of DNA strand exchange in homologous recombination. *DNA Repair (Amst)*, **9**, 1264–1272.
8. Esta,A., Ma,E., Dupaigne,P., Maloisel,L., Guerois,R., Le Cam,E., Veaute,X. and Coic,E. (2013) Rad52 sumoylation prevents the toxicity of unproductive Rad51 filaments independently of the anti-recombinase Srs2. *PLoS Genet.*, **9**, e1003833.
9. Krejci,L., Altmannova,V., Spirek,M. and Zhao,X. (2012) Homologous recombination and its regulation. *Nucleic Acids Res.*, **40**, 5795–5818.
10. Gaines,W.A., Godin,S.K., Kabbinavar,F.F., Rao,T., VanDemark,A.P., Sung,P. and Bernstein,K.A. (2015) Promotion of presynaptic filament assembly by the ensemble of *S. cerevisiae* Rad51 paralogues with Rad52. *Nat. Commun.*, **6**, 7834.
11. Sung,P. (1997) Yeast Rad55 and Rad57 proteins form a heterodimer that functions with replication protein A to promote DNA strand exchange by Rad51 recombinase. *Genes Dev.*, **11**, 1111–1121.
12. Sugawara,N., Wang,X. and Haber,J.E. (2003) In vivo roles of Rad52, Rad54, and Rad55 proteins in Rad51-mediated recombination. *Mol. Cell*, **12**, 209–219.
13. Shinohara,A. and Ogawa,T. (1998) Stimulation by Rad52 of yeast Rad51-mediated recombination. *Nature*, **391**, 404–407.
14. Sasanuma,H., Tawaramoto,M.S., Lao,J.P., Hosaka,H., Sanda,E., Suzuki,M., Yamashita,E., Hunter,N., Shinohara,M., Nakagawa,A. *et al.* (2013) A new protein complex promoting the assembly of Rad51 filaments. *Nat. Commun.*, **4**, 1676.
15. She,Z., Gao,Z.Q., Liu,Y., Wang,W.J., Liu,G.F., Shtykova,E.V., Xu,J.H. and Dong,Y.H. (2012) Structural and SAXS analysis of the budding yeast SHU-complex proteins. *FEBS Lett.*, **586**, 2306–2312.
16. Tao,Y., Li,X., Liu,Y., Ruan,J., Qi,S., Niu,L. and Teng,M. (2012) Structural analysis of Shu proteins reveals a DNA binding role essential for resisting damage. *J. Biol. Chem.*, **287**, 20231–20239.
17. Martin,V., Chahwan,C., Gao,H., Blais,V., Wohlschlegel,J., Yates,J.R., McGowan,C.H. and Russell,P. (2006) Sws1 is a conserved regulator of homologous recombination in eukaryotic cells. *EMBO J.*, **25**, 2564–2574.
18. Godin,S.K., Meslin,C., Kabbinavar,F., Bratton-Palmer,D.S., Hornack,C., Mihalevic,M.J., Yoshida,K., Sullivan,M., Clark,N.L. and Bernstein,K.A. (2015) Evolutionary and functional analysis of the invariant SWIM domain in the conserved Shu2/SWS1 protein

family from *Saccharomyces cerevisiae* to *Homo sapiens*. *Genetics*, **199**, 1023–1033.
19. Shor,E., Weinstein,J. and Rothstein,R. (2005) A genetic screen for top3 suppressors in *Saccharomyces cerevisiae* identifies *SHU1, SHU2, PSY3* and *CSM2*: four genes involved in error-free DNA repair. *Genetics*, **169**, 1275–1289.
20. Godin,S., Wier,A., Kabbinavar,F., Bratton-Palmer,D.S., Ghodke,H., Van Houten,B., VanDemark,A.P. and Bernstein,K.A. (2013) The Shu complex interacts with Rad51 through the Rad51 paralogues Rad55-Rad57 to mediate error-free recombination. *Nucleic Acids Res.*, **41**, 4525–4534.
21. Xu,X., Ball,L., Chen,W., Tian,X., Lambrecht,A., Hanna,M. and Xiao,W. (2013) The yeast Shu complex utilizes homologous recombination machinery for error-free lesion bypass via physical interaction with a Rad51 paralogue. *PLoS One*, **8**, e81371.
22. Ball,L.G., Zhang,K., Cobb,J.A., Boone,C. and Xiao,W. (2009) The yeast Shu complex couples error-free post-replication repair to homologous recombination. *Mol. Microbiol.*, **73**, 89–102.
23. Huang,M.E., Rio,A.G., Nicolas,A. and Kolodner,R.D. (2003) A genomewide screen in *Saccharomyces cerevisiae* for genes that suppress the accumulation of mutations. *Proc. Natl. Acad. Sci. U.S.A.*, **100**, 11529–11534.
24. Mankouri,H.W., Ngo,H.P. and Hickson,I.D. (2007) Shu proteins promote the formation of homologous recombination intermediates that are processed by Sgs1-Rmi1-Top3. *Mol. Biol. Cell*, **18**, 4062–4073.
25. Tercero,J.A. and Diffley,J.F. (2001) Regulation of DNA replication fork progression through damaged DNA by the Mec1/Rad53 checkpoint. *Nature*, **412**, 553–557.
26. Boiteux,S. and Laval,J. (1982) Mutagenesis by alkylating agents: coding properties for DNA polymerase of poly (dC) template containing 3-methylcytosine. *Biochimie*, **64**, 637–641.
27. Larson,K., Sahm,J., Shenkar,R. and Strauss,B. (1985) Methylation-induced blocks to in vitro DNA replication. *Mutat. Res.*, **150**, 77–84.
28. Yang,Y., Gordenin,D.A. and Resnick,M.A. (2010) A single-strand specific lesion drives MMS-induced hyper-mutability at a double-strand break in yeast. *DNA Repair (Amst)*, **9**, 914–921.
29. Boiteux,S. and Jinks-Robertson,S. (2013) DNA repair mechanisms and the bypass of DNA damage in *Saccharomyces cerevisiae*. *Genetics*, **193**, 1025–1064.
30. Bjoras,M., Klungland,A., Johansen,R.F. and Seeberg,E. (1995) Purification and properties of the alkylation repair DNA glycosylase encoded the *MAG* gene from *Saccharomyces cerevisiae*. *Biochemistry*, **34**, 4577–4582.
31. Chen,J., Derfler,B., Maskati,A. and Samson,L. (1989) Cloning a eukaryotic DNA glycosylase repair gene by the suppression of a DNA repair defect in *Escherichia coli*. *Proc. Natl. Acad. Sci. U.S.A.*, **86**, 7961–7965.
32. Lee,C.Y., Delaney,J.C., Kartalou,M., Lingaraju,G.M., Maor-Shoshani,A., Essigmann,J.M. and Samson,L.D. (2009) Recognition and processing of a new repertoire of DNA substrates by human 3-methyladenine DNA glycosylase (AAG). *Biochemistry*, **48**, 1850–1861.
33. Xiao,W., Chow,B.L., Hanna,M. and Doetsch,P.W. (2001) Deletion of the *MAG1* DNA glycosylase gene suppresses alkylation-induced killing and mutagenesis in yeast cells lacking AP endonucleases. *Mutat. Res.*, **487**, 137–147.
34. Scharer,O.D. and Jiricny,J. (2001) Recent progress in the biology, chemistry and structural biology of DNA glycosylases. *Bioessays*, **23**, 270–281.
35. Boiteux,S. and Guillet,M. (2004) Abasic sites in DNA: repair and biological consequences in *Saccharomyces cerevisiae*. *DNA Repair (Amst)*, **3**, 1–12.
36. Fortini,P. and Dogliotti,E. (2007) Base damage and single-strand break repair: mechanisms and functional significance of short- and long-patch repair subpathways. *DNA Repair (Amst)*, **6**, 398–409.
37. Wu,X. and Wang,Z. (1999) Relationships between yeast Rad27 and Apn1 in response to apurinic/apyrimidinic (AP) sites in DNA. *Nucleic Acids Res.*, **27**, 956–962.
38. Ma,W., Westmoreland,J.W., Gordenin,D.A. and Resnick,M.A. (2011) Alkylation base damage is converted into repairable double-strand breaks and complex intermediates in G2 cells lacking AP endonuclease. *PLoS Genet.*, **7**, e1002059.
39. Sherman,F., Fink,G.R. and Hicks,J.B. (1986) *Methods in Yeast Genetics*. Cold Spring Harbor Laboratory Press, NY.
40. Janke,C., Magiera,M.M., Rathfelder,N., Taxis,C., Reber,S., Maekawa,H., Moreno-Borchart,A., Doenges,G., Schwob,E., Schiebel,E. *et al.* (2004) A versatile toolbox for PCR-based tagging of yeast genes: new fluorescent proteins, more markers and promoter substitution cassettes. *Yeast*, **21**, 947–962.
41. Wach,A., Brachat,A., Alberti-Segui,C., Rebischung,C. and Philippsen,P. (1997) Heterologous *HIS3* marker and GFP reporter modules for PCR-targeting in *Saccharomyces cerevisiae*. *Yeast*, **13**, 1065–1075.
42. Lea,D.E. and Coulson,C.A. (1949) The distribution of the numbers of mutants in bacterial populations. *J. Genetics*, **49**, 264–285.
43. Hall,B.M., Ma,C.X., Liang,P. and Singh,K.K. (2009) Fluctuation analysis CalculatOR: a web tool for the determination of mutation rate using Luria-Delbruck fluctuation analysis. *Bioinformatics*, **25**, 1564–1565.
44. Bohm,S., Mihalevic,M.J., Casal,M.A. and Bernstein,K.A. (2015) Disruption of SUMO-targeted ubiquitin ligases Slx5-Slx8/RNF4 alters RecQ-like helicase Sgs1/BLM localization in yeast and human cells. *DNA Repair (Amst)*, **26**, 1–14.
45. Herzberg,K., Bashkirov,V.I., Rolfsmeier,M., Haghnazari,E., McDonald,W.H., Anderson,S., Bashkirova,E.V., Yates,J.R. 3rd and Heyer,W.D. (2006) Phosphorylation of Rad55 on serines 2, 8, and 14 is required for efficient homologous recombination in the recovery of stalled replication forks. *Mol. Cell. Biol.*, **26**, 8396–8409.
46. Wu,H.I., Brown,J.A., Dorie,M.J., Lazzeroni,L. and Brown,J.M. (2004) Genome-wide identification of genes conferring resistance to the anticancer agents cisplatin, oxaliplatin, and mitomycin C. *Cancer Res.*, **64**, 3940–3948.
47. St Onge,R.P., Mani,R., Oh,J., Proctor,M., Fung,E., Davis,R.W., Nislow,C., Roth,F.P. and Giaever,G. (2007) Systematic pathway analysis using high-resolution fitness profiling of combinatorial gene deletions. *Nat. Genet.*, **39**, 199–206.
48. Glassner,B.J., Rasmussen,L.J., Najarian,M.T., Posnick,L.M. and Samson,L.D. (1998) Generation of a strong mutator phenotype in yeast by imbalanced base excision repair. *Proc. Natl. Acad. Sci. U.S.A.*, **95**, 9997–10002.
49. Hendricks,C.A., Razlog,M., Matsuguchi,T., Goyal,A., Brock,A.L. and Engelward,B.P. (2002) The *S. cerevisiae* Mag1 3-methyladenine DNA glycosylase modulates susceptibility to homologous recombination. *DNA Repair (Amst)*, **1**, 645–659.
50. Dong,Z. and Fasullo,M. (2003) Multiple recombination pathways for sister chromatid exchange in Saccharomyces cerevisiae: role of *RAD1* and the *RAD52* epistasis group genes. *Nucleic Acids Res.*, **31**, 2576–2585.
51. Ma,W., Resnick,M.A. and Gordenin,D.A. (2008) Apn1 and Apn2 endonucleases prevent accumulation of repair-associated DNA breaks in budding yeast as revealed by direct chromosomal analysis. *Nucleic Acids Res.*, **36**, 1836–1846.
52. Degtyareva,N.P., Heyburn,L., Sterling,J., Resnick,M.A., Gordenin,D.A. and Doetsch,P.W. (2013) Oxidative stress-induced mutagenesis in single-strand DNA occurs primarily at cytosines and is DNA polymerase zeta-dependent only for adenines and guanines. *Nucleic Acids Res.*, **41**, 8995–9005.
53. Swanson,R.L., Morey,N.J., Doetsch,P.W. and Jinks-Robertson,S. (1999) Overlapping specificities of base excision repair, nucleotide excision repair, recombination, and translesion synthesis pathways for DNA base damage in Saccharomyces cerevisiae. *Mol. Cell Biol.*, **19**, 2929–2935.
54. Heacock,M., Poltoratsky,V., Prasad,R. and Wilson,S.H. (2012) Evidence for abasic site sugar phosphate-mediated cytotoxicity in alkylating agent treated Saccharomyces cerevisiae. *PLoS One*, **7**, e47945.
55. Fu,D., Calvo,J.A. and Samson,L.D. (2012) Balancing repair and tolerance of DNA damage caused by alkylating agents. *Nat. Rev. Cancer*, **12**, 104–120.
56. Paulovich,A.G. and Hartwell,L.H. (1995) A checkpoint regulates the rate of progression through S phase in *S. cerevisiae* in response to DNA damage. *Cell*, **82**, 841–847.
57. Shirahige,K., Hori,Y., Shiraishi,K., Yamashita,M., Takahashi,K., Obuse,C., Tsurimoto,T. and Yoshikawa,H. (1998) Regulation of DNA-replication origins during cell-cycle progression. *Nature*, **395**, 618–621.

58. Monti,P., Foggetti,G., Menichini,P., Inga,A., Gold,B. and Fronza,G. (2014) Comparison of the biological effects of MMS and Me-lex, a minor groove methylating agent: clarifying the role of N3-methyladenine. *Mutat. Res.*, **759**, 45–51.
59. Popoff,S.C., Spira,A.I., Johnson,A.W. and Demple,B. (1990) Yeast structural gene (APN1) for the major apurinic endonuclease: homology to *Escherichia coli* endonuclease IV. *Proc. Natl. Acad. Sci. U.S.A.*, **87**, 4193–4197.
60. Johnson,R.E., Torres-Ramos,C.A., Izumi,T., Mitra,S., Prakash,S. and Prakash,L. (1998) Identification of *APN2*, the *Saccharomyces cerevisiae* homolog of the major human AP endonuclease HAP1, and its role in the repair of abasic sites. *Genes Dev.*, **12**, 3137–3143.
61. Demple,B., Johnson,A. and Fung,D. (1986) Exonuclease III and endonuclease IV remove 3′ blocks from DNA synthesis primers in H2O2-damaged *Escherichia coli*. *Proc. Natl. Acad. Sci. U.S.A.*, **83**, 7731–7735.
62. Hansen,R.J., Friedberg,E.C. and Reagan,M.S. (2000) Sensitivity of a *S. cerevisiae RAD27* deletion mutant to DNA-damaging agents and in vivo complementation by the human FEN-1 gene. *Mutat. Res.*, **461**, 243–248.
63. Reagan,M.S., Pittenger,C., Siede,W. and Friedberg,E.C. (1995) Characterization of a mutant strain of *Saccharomyces cerevisiae* with a deletion of the *RAD27* gene, a structural homolog of the *RAD2* nucleotide excision repair gene. *J. Bacteriol.*, **177**, 364–371.
64. Mozlin,A.M., Fung,C.W. and Symington,L.S. (2008) Role of the *Saccharomyces cerevisiae* Rad51 paralogs in sister chromatid recombination. *Genetics*, **178**, 113–126.
65. Meindl,A., Hellebrand,H., Wiek,C., Erven,V., Wappenschmidt,B., Niederacher,D., Freund,M., Lichtner,P., Hartmann,L., Schaal,H. *et al.* (2010) Germline mutations in breast and ovarian cancer pedigrees establish RAD51C as a human cancer susceptibility gene. *Nat. Genet.*, **42**, 410–414.
66. Vaz,F., Hanenberg,H., Schuster,B., Barker,K., Wiek,C., Erven,V., Neveling,K., Endt,D., Kesterton,I., Autore,F. *et al.* (2010) Mutation of the RAD51C gene in a Fanconi anemia-like disorder. *Nat. Genet.*, **42**, 406–409.
67. Meira,L.B., Calvo,J.A., Shah,D., Klapacz,J., Moroski-Erkul,C.A., Bronson,R.T. and Samson,L.D. (2014) Repair of endogenous DNA base lesions modulate lifespan in mice. *DNA Repair (Amst)*, **21**, 78–86.
68. Bryant,H.E., Schultz,N., Thomas,H.D., Parker,K.M., Flower,D., Lopez,E., Kyle,S., Meuth,M., Curtin,N.J. and Helleday,T. (2005) Specific killing of BRCA2-deficient tumours with inhibitors of poly(ADP-ribose) polymerase. *Nature*, **434**, 913–917.
69. Auerbach,P.A. and Demple,B. (2010) Roles of Rev1, Pol zeta, Pol32 and Pol eta in the bypass of chromosomal abasic sites in *Saccharomyces cerevisiae*. *Mutagenesis*, **25**, 63–69.